

Sparse Nonnegative Tensor Factorization and Completion with Noisy Observations

Xiongjun Zhang and Michael K. Ng

Abstract

In this paper, we study the sparse nonnegative tensor factorization and completion problem from partial and noisy observations for third-order tensors. Because of sparsity and nonnegativity, the underlying tensor is decomposed into the tensor-tensor product of one sparse nonnegative tensor and one nonnegative tensor. We propose to minimize the sum of the maximum likelihood estimate for the observations with nonnegativity constraints and the tensor ℓ_0 norm for the sparse factor. We show that the error bounds of the estimator of the proposed model can be established under general noise observations. The detailed error bounds under specific noise distributions including additive Gaussian noise, additive Laplace noise, and Poisson observations can be derived. Moreover, the minimax lower bounds are shown to be matched with the established upper bounds up to a logarithmic factor of the sizes of the underlying tensor. These theoretical results for tensors are better than those obtained for matrices, and this illustrates the advantage of the use of nonnegative sparse tensor models for completion and denoising. Numerical experiments are provided to validate the superiority of the proposed tensor-based method compared with the matrix-based approach.

Index Terms

Sparse nonnegative tensor factorization and completion, tensor-tensor product, maximum likelihood estimate, error bound.

I. INTRODUCTION

With the rapid development of computer technique, multi-dimensional data, which is also known as tensors [1], has received much attention in various application fields, such as data mining [2, 3], signal and image processing [4–7], and neuroscience [8]. Many underlying tensor data is nonnegative due to their physical meaning such as the pixels of images. An efficient approach to exploit the intrinsic structure of a nonnegative tensor is tensor factorization, which can explore its hidden information. Moreover, the underlying tensor data may also suffer from missing entries and noisy corruptions during its acquiring process. In this paper, we focus on the sparse nonnegative tensor factorization (NTF) and completion problem from partial and noisy observations, where the observed entries are corrupted by general noise such as additive Gaussian noise, additive Laplace noise, and Poisson observations.

Tensors arise in a variety of real-world applications that can represent the multi-dimensional correlation of the underlying tensor data, e.g., the spatial and spectral dimensions for hyperspectral images and the spatial and time dimensions for video data. In particular, for second-order

The work of X. Zhang was partially supported by the National Natural Science Foundation of China under grants 11801206, 11871025, Hubei Provincial Natural Science Foundation of China under grant 2018CFB105, and Fundamental Research Funds for the Central Universities under grant CCNU19ZN017. The work of M. K. Ng was partially supported by the HKRGC GRF 12306616, 12200317, 12300218, 12300519 and 17201020, and HKU Grant 104005583.

X. Zhang is with the School of Mathematics and Statistics and Hubei Key Laboratory of Mathematical Sciences, Central China Normal University, Wuhan 430079, China (e-mail: xjzhang@mail.ccnu.edu.cn).

M. K. Ng is with the Department of Mathematics, The University of Hong Kong, Pokfulam, Hong Kong (e-mail: mng@maths.hku.hk).

tensors, NTF reduces to nonnegative matrix factorization (NMF), which can extract meaningful features and has a wide variety of practical applications in scientific and engineering areas, see [9–13] and references therein. Here the order of a tensor is the number of dimensions, also known as ways or modes [1]. It has been demonstrated that NMF is able to learn localized features with obvious interpretations [10]. Moreover, Gillis [14] proposed a sparse NMF model with a sparse factor, which provably led to optimal and sparse solutions under a separability assumption. Gao et al. [15] showed that sparse NMF can improve molecular cancer class discovery than the direct application of the basic NMF. Zhi et al. [16] also showed that sparse NMF provided better facial representations and achieved higher recognition rates than NMF for facial expression recognition. More applications about the advantages of sparse NMF over NMF can be referred to [17–19]. Besides, Soni et al. [20] proposed a general class of matrix completion tasks with noisy observations, which could reduce to sparse NMF when the underlying factor matrices are nonnegative and all entries of the noisy matrix are observed. They showed that the error bounds of estimators of sparse NMF are lower than those of NMF [20]. Furthermore, Sambasivan et al. [21] derived the minimax lower bounds of the expected per-element square error under general noise observations.

Due to exploiting the intrinsic structure of the underlying tensor data, which contains correlation in different modes, NTF has also been widely applied in a variety of fields, see, e.g., [22–26]. There are some popular NTF approaches, such as nonnegative Tucker decomposition [27], nonnegative CANDECOMP/PARAFAC (CP) decomposition [26], nonnegative tensor train decomposition [28], which are derived by different applications, see also [1, 29]. For example, Xu [30] proposed an alternating proximal gradient method for sparse nonnegative Tucker decomposition, while it is only efficient for additive Gaussian noise. Qi et al. [31] utilized Tucker decomposition to establish the redundant basis of the space of multi-linear maps with the sparsity constraint, and further proposed multi-dimensional synthesis/analysis sparse models to represent multi-dimensional signals effectively and efficiently. Moreover, Mørup et al. [24] showed that sparse nonnegative Tucker decomposition yields a parts-based representation as seen in NMF for two-way data, which is a simpler and more interpretable decomposition than the standard nonnegative Tucker decomposition for multi-dimensional data. Furthermore, they showed that sparse nonnegative Tucker decomposition can help reduce ambiguities by imposing constraints of sparseness in the decomposition for model selection and component identification. For nonnegative CP decomposition, Veganzones et al. [26] proposed a novel compression-based nonnegative CP decomposition without sparse constraints for blind spectral unmixing of hyperspectral images, which was only utilized for the observations with additive Gaussian noise. Kim et al. [32] proposed a sparse CP decomposition model, which improved the analysis and inference of multi-dimensional data for dimensionality reduction, feature selection as well as signal recovery.

Another kind of NTF is based on the recently proposed tensor-tensor product [33], whose algebra operators have been proposed and studied for third-order tensors [33, 34] and then generalized to higher-order tensors [35] and transformed tensor-tensor product [36]. Besides, Kilmer et al. [33] established the framework of tensor singular value decomposition (SVD). This kind of tensor-tensor product and tensor SVD has been applied in a great number of areas such as facial recognition [37], tensor completion [38–42], and image processing [43, 44]. Recently, this kind of sparse NTF models have been proposed and studied on dictionary learning problems, e.g., tomographic image reconstruction [45], image compression and image deblurring [46]. The sparse factor in this kind of NTF with tensor-tensor product is due to the sparse representation of patched-dictionary elements for tensor dictionary learning [45]. One needs to learn a nonnegative

tensor patch dictionary from training data, which is to solve a sparse NTF problem with tensor-tensor product. It was demonstrated that the tensor-based dictionary learning algorithm exhibits better performance than the matrix-based method in terms of approximation accuracy. However, there is no theoretical result about the error bounds of nonnegative sparse tensor factorization models. Both different noise settings and missing values are not studied in the literature.

In this paper, we propose a sparse NTF and completion model with tensor-tensor product from partial and noisy observations for third-order tensors, where the observations are corrupted by a general class of noise models. The proposed model consists of a data-fitting term for the observations and the tensor ℓ_0 norm for the sparse factor, where the two tensor factors operated by tensor-tensor product are nonnegative and the data-fitting term is derived by the maximum likelihood estimate. Theoretically, we show that the error bounds of the estimator of the proposed model can be established under general noise observations. The detailed error bounds under specific noise distributions including additive Gaussian noise, additive Laplace noise, and Poisson observations can be derived. Moreover, the minimax lower bounds are shown to be matched with the established upper bounds up to a logarithmic factor of the sizes of the underlying tensor. These theoretical results for tensors are better than those obtained for matrices [20], and this illustrates the advantage of the use of nonnegative sparse tensor models for completion and denoising. Then an alternating direction method of multipliers (ADMM) based algorithm [47, 48] is developed to solve the general noise observation models. Numerical examples are presented to show the performance of the proposed sparse NTF and completion is better than that of the matrix-based factorization [20].

The main contributions of this paper are summarized as follows. (1) Based on tensor-tensor product, a sparse NTF and completion model from partial and noisy observations is proposed under general noise distributions. (2) The upper bounds of the estimators of the proposed model are established under general noise observations. Then the upper bounds are specialized to the widely used noise observations including additive Gaussian noise, additive Laplace noise, and Poisson observations. (3) The minimax lower bounds are derived for the previous noise observations, which match the upper bounds with a logarithmic factor for different noise models. (4) An ADMM based algorithm is developed to solve the resulting model. And numerical experiments are presented to demonstrate the effectiveness of the proposed tensor-based method compared with the matrix-based method in [20].

The rest of this paper is organized as follows. Some notation and notions are provided in Section II. We propose a sparse NTF and completion model based on tensor-tensor product from partial and noisy observations in Section III, where the observations are corrupted by a general class of noise. In Section IV, the upper bounds of estimators of the proposed model are established, which are specialized to three widely used noise models including additive Gaussian noise, additive Laplace noise, and Poisson observations. Then the minimax lower bounds are also derived for the previous observation models in Section V. An ADMM based algorithm is developed to solve the resulting model in Section VI. Numerical experiments are reported to validate the effectiveness of the proposed method in Section VII. Finally, the conclusions and future work are given in Section VIII. All proofs of the theoretical results are delegated to the appendix.

II. PRELIMINARIES

Throughout this paper, \mathbb{R} represents the space with real numbers. $\mathbb{R}_+^{n_1 \times n_2 \times n_3}$ denotes the tensor space that all elements of the tensors are nonnegative. Scalars are represented by lowercase letters, e.g., x . Vectors and matrices are represented by lowercase boldface letters and uppercase

boldface letters, respectively, e.g., \mathbf{x} and \mathbf{X} . Tensors are denoted by capital Euler script letters, e.g., \mathcal{X} . The (i, j, k) th entry of a tensor \mathcal{X} is denoted as \mathcal{X}_{ijk} . The i th frontal slice of a tensor \mathcal{X} is a matrix denoted by $\mathbf{X}^{(i)}$, which is a matrix by fixing the third index and vary the first two indexes of \mathcal{X} .

The ℓ_2 norm of a vector $\mathbf{x} \in \mathbb{R}^n$, denoted by $\|\mathbf{x}\|$, is defined as $\|\mathbf{x}\| = \sqrt{\sum_{i=1}^n x_i^2}$, where x_i is the i th entry of \mathbf{x} . The tensor ℓ_∞ norm of a tensor \mathcal{X} is defined as $\|\mathcal{X}\|_\infty = \max_{i,j,k} |\mathcal{X}_{ijk}|$. The tensor ℓ_0 norm of \mathcal{X} , denoted by $\|\mathcal{X}\|_0$, is defined as the count of all nonzero entries of \mathcal{X} . The inner product of two tensors $\mathcal{X}, \mathcal{Y} \in \mathbb{R}^{n_1 \times n_2 \times n_3}$ is defined as $\langle \mathcal{X}, \mathcal{Y} \rangle = \sum_{i=1}^{n_3} \langle \mathbf{X}^{(i)}, \mathbf{Y}^{(i)} \rangle$, where $\langle \mathbf{X}^{(i)}, \mathbf{Y}^{(i)} \rangle = \text{tr}((\mathbf{X}^{(i)})^T \mathbf{Y}^{(i)})$. Here \cdot^T and $\text{tr}(\cdot)$ denote the transpose and the trace of a matrix, respectively. The tensor Frobenius norm of \mathcal{X} is defined as $\|\mathcal{X}\|_F = \sqrt{\langle \mathcal{X}, \mathcal{X} \rangle}$.

Let $p_{x_1}(y_1)$ and $p_{x_2}(y_2)$ be the probability density functions or probability mass functions with respect to the random variables y_1 and y_2 with parameters x_1 and x_2 , respectively. The Kullback-Leibler (KL) divergence of $p_{x_1}(y_1)$ from $p_{x_2}(y_2)$ is defined as

$$D(p_{x_1}(y_1) || p_{x_2}(y_2)) = \mathbb{E}_{p_{x_1}(y_1)} \left[\log \frac{p_{x_1}(y_1)}{p_{x_2}(y_2)} \right].$$

The Hellinger affinity between $p_{x_1}(y_1)$ and $p_{x_2}(y_2)$ is defined as

$$H(p_{x_1}(y_1) || p_{x_2}(y_2)) = \mathbb{E}_{p_{x_1}} \left[\sqrt{\frac{p_{x_2}(y_2)}{p_{x_1}(y_1)}} \right] = \mathbb{E}_{p_{x_2}} \left[\sqrt{\frac{p_{x_1}(y_1)}{p_{x_2}(y_2)}} \right].$$

The joint distributions of higher-order and multi-dimensional variables, denoted by $p_{\mathcal{X}_1}(\mathcal{Y}), p_{\mathcal{X}_2}(\mathcal{Y})$, are the joint distributions of the vectorization of the tensors. Then the KL divergence of $p_{\mathcal{X}_1}(\mathcal{Y})$ from $p_{\mathcal{X}_2}(\mathcal{Y})$ is defined as

$$D(p_{\mathcal{X}_1}(\mathcal{Y}) || p_{\mathcal{X}_2}(\mathcal{Y})) := \sum_{i,j,k} D(p_{\mathcal{X}_{ijk}}(\mathcal{Y}_{ijk}) || p_{\mathcal{Y}_{ijk}}(\mathcal{Y}_{ijk})),$$

and its Hellinger affinity is defined as

$$H(p_{\mathcal{X}_1}(\mathcal{Y}) || p_{\mathcal{X}_2}(\mathcal{Y})) := \prod_{i,j,k} H(p_{\mathcal{X}_{ijk}}(\mathcal{Y}_{ijk}), p_{\mathcal{Y}_{ijk}}(\mathcal{Y}_{ijk})).$$

Now we define the tensor-tensor product between two third-order tensors [33].

Definition 2.1: [33, Definition 3.1] Let $\mathcal{X} \in \mathbb{R}^{n_1 \times n_2 \times n_3}$ and $\mathcal{Y} \in \mathbb{R}^{n_2 \times n_4 \times n_3}$. The tensor-tensor product, denoted as $\mathcal{X} \diamond \mathcal{Y}$, is an $n_1 \times n_4 \times n_3$ tensor defined by

$$\mathcal{X} \diamond \mathcal{Y} := \text{Fold}(\text{Circ}(\text{Unfold}(\mathcal{X})) \cdot \text{Unfold}(\mathcal{Y})),$$

where

$$\text{Unfold}(\mathcal{X}) = \begin{pmatrix} \mathbf{X}^{(1)} \\ \mathbf{X}^{(2)} \\ \vdots \\ \mathbf{X}^{(n_3)} \end{pmatrix}, \text{Fold} \begin{pmatrix} \mathbf{X}^{(1)} \\ \mathbf{X}^{(2)} \\ \vdots \\ \mathbf{X}^{(n_3)} \end{pmatrix} = \mathcal{X}, \text{Circ} \begin{pmatrix} \mathbf{X}^{(1)} \\ \mathbf{X}^{(2)} \\ \vdots \\ \mathbf{X}^{(n_3)} \end{pmatrix} = \begin{pmatrix} \mathbf{X}^{(1)} & \mathbf{X}^{(n_3)} & \dots & \mathbf{X}^{(2)} \\ \mathbf{X}^{(2)} & \mathbf{X}^{(1)} & \dots & \mathbf{X}^{(3)} \\ \vdots & \vdots & & \vdots \\ \mathbf{X}^{(n_3)} & \mathbf{X}^{(n_3-1)} & \dots & \mathbf{X}^{(1)} \end{pmatrix}.$$

By the block circulate structure, the tensor-tensor product of two third-order tensors can be implemented efficiently by fast Fourier transform [33].

Definition 2.2: [33] The transpose of a tensor $\mathcal{X} \in \mathbb{R}^{n_1 \times n_2 \times n_3}$, is the tensor $\mathcal{X}^T \in \mathbb{R}^{n_2 \times n_1 \times n_3}$ obtained by transposing each of the frontal slices and then reversing the order of transposed frontal slices 2 through n_3 , i.e.,

$$(\mathcal{X}^T)^{(1)} = (\mathbf{X}^{(1)})^T, (\mathcal{X}^T)^{(i)} = (\mathbf{X}^{(n_3+2-i)})^T, i = 2, \dots, n_3.$$

Definition 2.3: [33, Definition 3.4] An $n \times n \times m$ identity tensor \mathcal{I} is the tensor whose first frontal slice is the $n \times n$ identity matrix, and whose other frontal slices are all zeros.

Definition 2.4: [33, Definition 3.5] A tensor $\mathcal{A} \in \mathbb{R}^{n \times n \times m}$ is said to have an inverse, denoted by $\mathcal{A}^{-1} \in \mathbb{R}^{n \times n \times m}$, if $\mathcal{A} \diamond \mathcal{A}^{-1} = \mathcal{A}^{-1} \diamond \mathcal{A} = \mathcal{I}$, where $\mathcal{I} \in \mathbb{R}^{n \times n \times m}$ is the identity tensor.

The proximal mapping of a closed proper function $f : \mathfrak{C} \rightarrow (-\infty, +\infty]$ is defined as

$$\text{Prox}_f(y) = \arg \min_{x \in \mathfrak{C}} \left\{ f(x) + \frac{1}{2} \|x - y\|^2 \right\},$$

where \mathfrak{C} is a finite-dimensional Euclidean space. Next we provide a brief summary of the notation used throughout this paper.

- $\lfloor x \rfloor$ is the integer part of x . $\lceil x \rceil$ is smallest integer that is larger or equal to x .
- Denote $m \vee n = \max\{m, n\}$ and $m \wedge n = \min\{m, n\}$.

III. SPARSE NTF AND COMPLETION VIA TENSOR-TENSOR PRODUCT

Let $\mathcal{X}^* \in \mathbb{R}_+^{n_1 \times n_2 \times n_3}$ be an unknown nonnegative tensor we aim to estimate, which admits a following nonnegative factorization:

$$\mathcal{X}^* = \mathcal{A}^* \diamond \mathcal{B}^*,$$

where $\mathcal{A}^* \in \mathbb{R}_+^{n_1 \times r \times n_3}$ and $\mathcal{B}^* \in \mathbb{R}_+^{r \times n_2 \times n_3}$ are prior unknown factor tensors with $r \leq \min\{n_1, n_2\}$. We assume that each entries of $\mathcal{X}^*, \mathcal{A}^*, \mathcal{B}^*$ are bounded, i.e.,

$$0 \leq \mathcal{X}_{ijk}^* \leq \frac{c}{2}, \quad 0 \leq \mathcal{A}_{ijk}^* \leq 1, \quad 0 \leq \mathcal{B}_{ijk}^* \leq b, \quad \forall i, j, k,$$

where $\frac{c}{2}$ is used for simplicity of subsequent analysis. We remark that the amplitude 1 of each entry \mathcal{A}_{ijk}^* of \mathcal{A}^* can be arbitrary. Besides, our focus is that the factor tensor \mathcal{B}^* is sparse.

However, only a noisy and incompleted version of the underlying tensor \mathcal{X}^* is available in practice. Let $\Omega \subseteq \{1, 2, \dots, n_1\} \times \{1, 2, \dots, n_2\} \times \{1, 2, \dots, n_3\}$ be a subset at which the entries of the observations \mathcal{Y} are collected. Denote $\mathcal{Y}_\Omega \in \mathbb{R}^m$ to be a vector such that the entries of \mathcal{Y} in the index Ω are vectorized into a vector by lexicographic order, where m is the number of observed entries. Assume that $n_1, n_2, n_3 \geq 2$ throughout this paper. Suppose that the location set Ω is generated according to an independent Bernoulli model with probability $\gamma = \frac{m}{n_1 n_2 n_3}$ (denoted by $\text{Bern}(\gamma)$), i.e., each index (i, j, k) belongs to Ω with probability γ , which is denoted as $\Omega \sim \text{Bern}(\gamma)$. Mathematically, the joint probability density function or probability mass function of observations \mathcal{Y}_Ω is given by

$$p_{\mathcal{X}_\Omega^*}(\mathcal{Y}_\Omega) := \prod_{(i,j,k) \in \Omega} p_{\mathcal{X}_{ijk}^*}(\mathcal{Y}_{ijk}). \quad (1)$$

By the maximum likelihood estimate, we propose the following sparse NTF and completion model with nonnegative constraints:

$$\tilde{\mathcal{X}}^\lambda \in \arg \min_{\mathcal{X} = \mathcal{A} \diamond \mathcal{B} \in \Gamma} \{-\log p_{\mathcal{X}_\Omega}(\mathcal{Y}_\Omega) + \lambda \|\mathcal{B}\|_0\}, \quad (2)$$

where $\lambda > 0$ is the regularization parameter and Γ is defined by

$$\Gamma := \{\mathcal{X} = \mathcal{A} \diamond \mathcal{B} : \mathcal{A} \in \mathfrak{L}, \mathcal{B} \in \mathfrak{D}, 0 \leq \mathcal{X}_{ijk} \leq c\}. \quad (3)$$

Here Γ is a countable set of estimates constructed as follows: First, let

$$\vartheta := 2^{\lceil \beta \log_2(n_1 \vee n_2) \rceil} \quad (4)$$

for a specified $\beta \geq 3$, we construct \mathcal{L} to be the set of all tensors $\mathcal{A} \in \mathbb{R}_+^{n_1 \times r \times n_3}$ whose entries are discretized to one of ϑ uniformly sized bins in the range $[0, 1]$, and \mathcal{D} to be the set of all tensors $\mathcal{B} \in \mathbb{R}_+^{r \times n_2 \times n_3}$ whose entries either take the value 0, or are discretized to one of ϑ uniformly sized bins in the range $[0, b]$.

Remark III.1: When all entries of \mathcal{Y} are observed and \mathcal{Y} is corrupted by additive Gaussian noise, the model (2) reduces to sparse NTF with tensor-tensor product, whose relaxation, replaced the tensor ℓ_0 norm by the tensor ℓ_1 norm, has been applied in patch-based dictionary learning for image data [45, 46].

Remark III.2: We do not specialize the noise in model (2), and just need the joint probability density function or probability mass function of observations in (1). In particular, our model can address the observations with some widely used noise distributions, such as additive Gaussian noise, additive Laplace noise, and Poisson observations.

IV. UPPER BOUNDS

In this section, we establish a general upper error bound of the sparse NTF and completion model from partial observations under a general class of noise in (2), and then derive the upper bounds of the special noise models including additive Gaussian noise, additive Laplace noise, and Poisson observations.

Now we establish the upper error bound of the estimator $\tilde{\mathcal{X}}^\lambda$ in (2), whose proof follows the line of the proof of [20, Theorem 1], see also [49, Theorem 3]. The key technique of this proof is the well-known Kraft-McMillan inequality [50, 51]. Then we construct the penalty of the underlying tensor \mathcal{X} with the tensor-tensor product of two nonnegative tensors, where one factor tensor is sparse.

Theorem 4.1: Suppose that $\kappa \geq \max_{\mathcal{X} \in \Gamma} \max_{i,j,k} D(p_{\mathcal{X}_{ijk}^*} \| p_{\mathcal{X}_{ijk}})$. Let $\Omega \sim \text{Bern}(\gamma)$, where $\gamma = \frac{m}{n_1 n_2 n_3}$ and $4 \leq m \leq n_1 n_2 n_3$. Then, for any $\lambda \geq 4(\beta + 2) \left(1 + \frac{2\kappa}{3}\right) \log((n_1 \vee n_2) \sqrt{n_3})$, the estimator $\tilde{\mathcal{X}}^\lambda$ in (2) satisfies

$$\begin{aligned} & \frac{\mathbb{E}_{\Omega, \mathcal{Y}_\Omega}[-2 \log H(p_{\tilde{\mathcal{X}}^\lambda}, p_{\mathcal{X}^*})]}{n_1 n_2 n_3} \\ & \leq 3 \min_{\mathcal{X} = \mathcal{A} \diamond \mathcal{B} \in \Gamma} \left\{ \frac{D(p_{\mathcal{X}^*} \| p_{\mathcal{X}})}{n_1 n_2 n_3} + \left(\lambda + \frac{8\kappa(\beta + 2) \log((n_1 \vee n_2) \sqrt{n_3})}{3} \right) \frac{r n_1 n_3 + \|\mathcal{B}\|_0}{m} \right\} \\ & \quad + \frac{8\kappa \log(m)}{m}. \end{aligned}$$

The detailed proof of Theorem 4.1 is left to Appendix A. From Theorem 4.1, we can observe that the upper bound of $\frac{\mathbb{E}_{\Omega, \mathcal{Y}_\Omega}[-2 \log H(p_{\tilde{\mathcal{X}}^\lambda}, p_{\mathcal{X}^*})]}{n_1 n_2 n_3}$ is of the order of $O\left(\frac{r n_1 n_3 + \|\mathcal{B}\|_0}{m} \log(n_1 \vee n_2)\right)$ if the KL divergence $D(p_{\mathcal{X}^*} \| p_{\mathcal{X}})$ is not too large in the set Γ . The explicit upper bounds with respect to $D(p_{\mathcal{X}^*} \| p_{\mathcal{X}})$ in Γ and κ will be given for the observations with special noise distributions.

Remark IV.1: For the upper error bounds of estimators of observations with special noise distributions, the main difference of proofs between the matrix case [20] and the tensor case is to establish the upper bound of $\min_{\mathcal{X} \in \Gamma} \|\mathcal{X}^* - \mathcal{X}\|_F^2$, where Γ is defined as (3). We need to estimate this bound based on the tensor-tensor product structure $\mathcal{X} = \mathcal{A} \diamond \mathcal{B} \in \Gamma$, which can be obtained by Lemma A.2. The key issue in Lemma A.2 is to construct the surrogates of entries of the two factor tensors $\mathcal{A}^*, \mathcal{B}^*$ in the set Γ , where $\mathcal{X}^* = \mathcal{A}^* \diamond \mathcal{B}^*$.

In the following subsections, we establish the upper error bounds of the estimators for the observations with three special noise models, including additive Gaussian noise, additive Laplace

noise, and Poisson observations. By Theorem 4.1, the main steps of proofs for the special noise models are to establish the lower bound of $-2\log(H(p_{\mathcal{X}^*}, p_{\tilde{\mathcal{X}}^\lambda}))$ and the upper bound of $\min_{\mathcal{X}=\mathcal{A} \circ \mathcal{B} \in \Gamma} D(p_{\mathcal{X}^*} \| p_{\mathcal{X}})$, respectively.

Before deriving the upper error bounds of the observations with special noise models, we fix the choices of β and λ based on Theorem 4.1, which are defined as follows:

$$\beta = \max \left\{ 3, 1 + \frac{\log(3rn_3^{1.5}b/c)}{\log(n_1 \vee n_2)} \right\}, \quad (5)$$

and

$$\lambda = 4(\beta + 2) \left(1 + \frac{2\kappa}{3} \right) \log(n_1 \vee n_2). \quad (6)$$

A. Additive Gaussian Noise

Assume that each entry of the underlying tensor is corrupted by independently additive zero-mean Gaussian noise with standard deviation $\sigma > 0$, that is

$$\mathcal{Y}_{ijk} = \mathcal{X}_{ijk}^* + \sigma^2 \epsilon_{ijk}, \quad (7)$$

where ϵ_{ijk} obeys the independently standard normal distribution (i.e., $\epsilon_{ijk} \sim N(0, 1)$) for any $(i, j, k) \in \Omega$. Then the observation \mathcal{Y}_Ω can be regarded as a vector and its joint probability density function in (1) is given as

$$p_{\mathcal{X}_\Omega^*}(\mathcal{Y}_\Omega) = \frac{1}{(2\pi\sigma^2)^{|\Omega|/2}} \exp \left(-\frac{1}{2\sigma^2} \|\mathcal{Y}_\Omega - \mathcal{X}_\Omega^*\|^2 \right), \quad (8)$$

where $|\Omega|$ denotes the number of entries of Ω , i.e., $|\Omega| = m$.

Now we establish the explicit upper error bound of the estimator in (2) with the observations \mathcal{Y}_Ω satisfying (7).

Proposition 4.1: Let $\Omega \sim \text{Bern}(\gamma)$, where $\gamma = \frac{m}{n_1 n_2 n_3}$ and $4 \leq m \leq n_1 n_2 n_3$. Assume that β and λ are defined as (5) and (6), respectively, where $\kappa = \frac{c^2}{2\sigma^2}$ in (6). Suppose that \mathcal{Y}_Ω satisfies (7). Then the estimator $\tilde{\mathcal{X}}^\lambda$ in (2) satisfies

$$\frac{\mathbb{E}_{\Omega, \mathcal{Y}_\Omega} [\|\tilde{\mathcal{X}}^\lambda - \mathcal{X}^*\|_F^2]}{n_1 n_2 n_3} \leq \frac{22c^2 \log(m)}{m} + 16(3\sigma^2 + 2c^2)(\beta + 2) \left(\frac{rn_1 n_3 + \|\mathcal{B}^*\|_0}{m} \right) \log(n_1 \vee n_2).$$

The detailed proof of Proposition 4.1 is left to Appendix B. From Proposition 4.1, we can see that the upper bound of $\frac{\mathbb{E}_{\Omega, \mathcal{Y}_\Omega} [\|\tilde{\mathcal{X}}^\lambda - \mathcal{X}^*\|_F^2]}{n_1 n_2 n_3}$ for the observations with additive Gaussian noise is of the order $O((\sigma^2 + c^2) \left(\frac{rn_1 n_3 + \|\mathcal{B}^*\|_0}{m} \right) \log(n_1 \vee n_2))$. Now we give a comparison with a matrix-based method in [20, Corollary 3] if we ignore the intrinsic structure of a tensor. Note that we cannot compare with the matrix-based method directly since the underlying data is the tensor form. However, we can stack these frontal slices of the underlying tensor (with size $n_1 \times n_2 \times n_3$) into a matrix, whose size is $n_1 n_3 \times n_2$. In this case, the estimator \mathcal{X}_1 obtained by the matrix-based method in [20, Corollary 3] satisfies

$$\frac{\mathbb{E}_{\Omega, \mathcal{Y}_\Omega} [\|\mathcal{X}_1 - \mathcal{X}^*\|_F^2]}{n_1 n_2 n_3} = O \left((\sigma^2 + c^2) \left(\frac{\tilde{r} n_1 n_3 + \|\mathcal{B}^*\|_0}{m} \right) \log((n_1 n_3) \vee n_2) \right), \quad (9)$$

where \tilde{r} is the rank of the resulting matrix. In particular, we choose \tilde{r} in the matrix-based method the same as r in the tensor-based method with tensor-tensor product. In real-world applications, $n_1 n_3 > n_2$ in general. For example, if n_3 denotes the frame in video datasets or

spectral dimensions in hyperspectral image datasets, n_3 is large. Therefore, if $n_1 n_3 > n_2$, the upper error bound of the matrix-based method in (9) is larger than that of the tensor-based method in Proposition 4.1. Especially, when $n_1 = n_2$, the logarithmic factor in Proposition 4.1 is $\log(n_1)$, while it is $\log(n_1 n_3) = \log(n_1) + \log(n_3)$ in (9).

Remark IV.2: We also compare the upper error bound with that of the noisy tensor completion in [52], which did not consider the sparse factor. The upper error bound of the estimator \mathcal{X}_t in [52, Theorem 1] satisfies

$$\frac{\|\mathcal{X}_t - \mathcal{X}^*\|_F^2}{n_1 n_2 n_3} \leq C_t (\sigma^2 \vee c^2) \left(\frac{r \max\{n_1, n_2\} n_3}{m} \right) \log((n_1 + n_2) n_3) \quad (10)$$

with high probability, where $C_t > 0$ is a constant. We note that the upper error bound of our method can be improved potentially when $n_2 > n_1$ and \mathcal{B}^* is sparse. In fact, the upper bound in Proposition 4.1 is of the order $O(\frac{r n_1 n_3}{m} \log(n_2))$, while the upper bound in [52] is of the order $O(\frac{r n_2 n_3}{m} \log((n_1 + n_2) n_3))$. Moreover, the two upper bounds roughly coincide except for the logarithmic factor when \mathcal{B}^* is not sparse, i.e., $\|\mathcal{B}^*\|_0 = r n_2 n_3$. However, when $n_1 \geq n_2$, the improvement of the upper bound of Proposition 4.1 is mainly on the logarithmic factor, which is much smaller than that of (10).

Remark IV.3: From Proposition 4.1, we know that the upper error bound decreases when the number of observations increases. In particular, when we observe all entries of \mathcal{Y} , i.e., $m = n_1 n_2 n_3$, Proposition 4.1 is the upper error bound of the sparse NTF model with tensor-tensor product in [45, 46], which has been used to construct a tensor patch dictionary prior for CT and facial images, respectively. This demonstrates that the upper error bound of sparse NTF with tensor-tensor product in [45, 46] is lower than that of sparse NMF in theory, where Soltani et al. [45] just showed the performance of sparse NTF with tensor-tensor product is better than that of sparse NMF in experiments.

B. Additive Laplace Noise

Suppose that each entry of the underlying tensor is corrupted by independently additive Laplace noise with the location parameter being zero and the diversity being $\tau > 0$ (denoted by $\text{Laplace}(0, \tau)$), that is

$$\mathcal{Y}_{ijk} = \mathcal{X}_{ijk}^* + \epsilon_{ijk}, \quad (11)$$

where $\epsilon_{ijk} \sim \text{Laplace}(0, \tau)$ for any $(i, j, k) \in \Omega$. Then the joint probability density function of the observation \mathcal{Y}_Ω is given by

$$p_{\mathcal{X}_\Omega^*}(\mathcal{Y}_\Omega) = \left(\frac{1}{2\tau} \right)^{|\Omega|} \exp \left(-\frac{\|\mathcal{Y}_\Omega - \mathcal{X}_\Omega^*\|_1}{\tau} \right). \quad (12)$$

Now we establish the upper error bound of estimators in (2) for the observations with additive Laplace noise.

Proposition 4.2: Let $\Omega \sim \text{Bern}(\gamma)$, where $\gamma = \frac{m}{n_1 n_2 n_3}$ and $4 \leq m \leq n_1 n_2 n_3$. Assume that \mathcal{Y}_Ω obeys to (7). Let β and λ be defined as (5) and (6), respectively, where $\kappa = \frac{c^2}{2\tau^2}$ in (6). Then the estimator $\tilde{\mathcal{X}}^\lambda$ in (2) satisfies

$$\begin{aligned} & \frac{\mathbb{E}_{\Omega, \mathcal{Y}_\Omega} [\|\tilde{\mathcal{X}}^\lambda - \mathcal{X}^*\|_F^2]}{n_1 n_2 n_3} \\ & \leq \frac{3c^2(2\tau + c)^2 \log(m)}{m\tau^2} + 2 \left(3 + \frac{c^2}{\tau^2} \right) (2\tau + c)^2 (\beta + 2) \left(\frac{r n_1 n_3 + \|\mathcal{B}^*\|_0}{m} \right) \log(n_1 \vee n_2). \end{aligned}$$

The detailed proof of Proposition 4.2 is delegated to Appendix C. Similar to the case of observations with additive Gaussian noise, we compare the upper error bound in Proposition 4.2 with that of [20, Corollary 5], which satisfies

$$\frac{\mathbb{E}_{\Omega, \mathcal{Y}_\Omega} [\|\mathcal{X}_2 - \mathcal{X}^*\|_F^2]}{n_1 n_2 n_3} = O \left((\tau + c)^2 \tau c \left(\frac{\tilde{r} n_1 n_3 + \|\mathcal{B}^*\|_0}{m} \right) \log((n_1 n_3) \vee n_2) \right), \quad (13)$$

where \mathcal{X}_2 is the estimator by the matrix-based method and \tilde{r} is the rank of the resulting matrix by matricizing the underlying tensor. Therefore, the difference of the upper error bounds between Proposition 4.2 and [20, Corollary 5] is mainly on the logarithmic factor. If $n_1 n_3 > n_2$, which holds in various real-world scenarios, the logarithmic factor in (13) is $\log(n_1 n_3)$, while it is $\log(n_1 \vee n_2)$ in Proposition 4.2. In particular, when $n_1 = n_2$, the logarithmic factor in (13) is $\log(n_1 n_3)$, while it is $\log(n_1)$ in Proposition 4.2.

C. Poisson Observations

Suppose that each entry of \mathcal{Y}_Ω follows a Poisson distribution, i.e.,

$$\mathcal{Y}_{ijk} = \text{Poisson}(\mathcal{X}_{ijk}^*), \quad \forall (i, j, k) \in \Omega, \quad (14)$$

where $y = \text{Poisson}(x)$ denotes that y obeys a Poisson distribution with parameter $x > 0$, each \mathcal{Y}_{ijk} is independent and $\mathcal{X}_{ijk}^* > 0$. The joint probability mass function of \mathcal{Y}_Ω is given as follows:

$$p_{\mathcal{X}_\Omega^*}(\mathcal{Y}_\Omega) = \prod_{(i,j,k) \in \Omega} \frac{(\mathcal{X}_{ijk}^*)^{\mathcal{Y}_{ijk}} \exp(-\mathcal{X}_{ijk}^*)}{\mathcal{Y}_{ijk}!}. \quad (15)$$

Now we establish the upper error bound of estimators in (2) for the observations obeying (14), which mainly bases on Theorem 4.1. The key step is to give the upper bound of $D(p_{\mathcal{X}^*} \| p_{\mathcal{X}})$.

Proposition 4.3: Let $\Omega \sim \text{Bern}(\gamma)$, where $\gamma = \frac{m}{n_1 n_2 n_3}$ and $4 \leq m \leq n_1 n_2 n_3$. Suppose that each entry of \mathcal{X}^* is positive, i.e., $\zeta := \min_{i,j,k} \mathcal{X}_{ijk}^* > 0$, and each entry of the candidate $\mathcal{X} \in \Gamma$ also satisfies $\mathcal{X}_{ijk} \geq \zeta$. Let β and λ be defined as (5) and (6), respectively, where $\kappa = c/\zeta$ in (6). Assume that \mathcal{Y}_Ω obeys to the distribution in (14). Then the estimator $\tilde{\mathcal{X}}^\lambda$ in (2) satisfies

$$\begin{aligned} & \frac{\mathbb{E}_{\Omega, \mathcal{Y}_\Omega} \|\tilde{\mathcal{X}}^\lambda - \mathcal{X}^*\|_F^2}{n_1 n_2 n_3} \\ & \leq \frac{4c^3(3 + 8 \log(m))}{\zeta m} + 48c \left(1 + \frac{4c^2}{3\zeta} \right) \frac{(\beta + 2) (r n_1 n_3 + \|\mathcal{B}^*\|_0) \log(n_1 \vee n_2)}{m}. \end{aligned}$$

We leave the detailed proof of Proposition 4.3 to Appendix D. Similar to the case of observations with additive Gaussian noise, we compare the upper error bound in Proposition 4.3 with that of the matrix-based method in [20, Corollary 6]. The resulting upper error bound of the matrix-based method is of the order

$$O \left(c \left(1 + \frac{c^2}{\zeta} \right) \left(\frac{\tilde{r} n_1 n_3 + \|\mathcal{B}^*\|_0}{m} \right) \log((n_1 n_3) \vee n_2) \right), \quad (16)$$

where \tilde{r} is the rank of the resulting matrix. The mainly difference of the upper error bounds between the tensor- and matrix-based methods is the logarithmic factor. Hence, if $n_1 n_3 > n_2$, which holds in various real-world scenarios, the logarithmic factor in (16) is $\log(n_1 n_3)$, while it is $\log(n_1 \vee n_2)$ in Proposition 4.3. In particular, the logarithmic factor in Proposition 4.3 is $\log(n_1)$ when $n_1 = n_2$.

Remark IV.4: The constants of the upper bound in Proposition 4.3 have some differences compared with the matrix-based method in [20, Corollary 6], which will also influence the recovery error in practice.

In addition, Cao et al. [53] proposed a matrix-based model for matrix completion with Poisson noise removal and established the upper error bound of the estimator, where the low-rank property is utilized by the upper bound of the nuclear norm of a matrix in a constrained set. The error bound of the estimator \mathcal{X}_3 in [53, Theorem 2] satisfies

$$\frac{\|\mathcal{X}_3 - \mathcal{X}^*\|_F^2}{n_1 n_2 n_3} \leq C_p \left(\frac{c^2 \sqrt{\tilde{r}}}{\zeta} \right) \frac{n_1 n_3 + n_2}{m} \log^{\frac{3}{2}}(n_1 n_2 n_3) \quad (17)$$

with high probability, where $C_p > 0$ is a given constant. Therefore, if $\log(n_1 n_2 n_3) > \tilde{r}$, the upper error bound of the tensor-based method has a great improvement on the logarithmic factor if \mathcal{B}^* is sparse. Specifically, when $n_1 = n_2$ and $\log(n_1 n_2 n_3) > \tilde{r}$, the logarithmic factor of (17) is $\log(n_1 n_2 n_3)$, while it is $\log(n_1)$ in Proposition 4.3. Recently, Zhang et al. [42] proposed a method for low-rank tensor completion with Poisson observations, which combined the transformed tensor nuclear norm ball constraint with maximum likelihood estimate. When $m \geq \frac{1}{2}(n_1 + n_2)n_3 \log(n_1 + n_2)$ and all entries of multi-rank of the underlying tensor \mathcal{X}^* are r_1 , the upper error bound of the estimator \mathcal{X}_{tc} in [42, Theorem 3.1] is

$$\frac{\|\mathcal{X}_{tc} - \mathcal{X}^*\|_F^2}{n_1 n_2 n_3} \leq C_{tc} n_3 \sqrt{\frac{(n_1 + n_2)r_1}{m}} \log(n_1 n_2 n_3)$$

with high probability, where $C_{tc} > 0$ is a given constant. In this case, since r_1 is small in general and $(n_1 + n_2)r_1/m < 1$, the upper error bound in [42, Theorem 3.1] is larger than that of Proposition 4.3.

V. MINIMAX LOWER BOUNDS

In this section, we study the sparse NTF and completion problem with incomplete and noisy observations, and establish the lower bounds on the minimax risk for the candidate estimator in the following set:

$$\mathfrak{U}(r, b, s) := \left\{ \mathcal{X} = \mathcal{A} \diamond \mathcal{B} \in \mathbb{R}_+^{n_1 \times n_2 \times n_3} : \mathcal{A} \in \mathbb{R}_+^{n_1 \times r \times n_3}, 0 \leq \mathcal{A}_{ijk} \leq 1, \right. \\ \left. \mathcal{B} \in \mathbb{R}_+^{r \times n_2 \times n_3}, 0 \leq \mathcal{B}_{ijk} \leq b, \|\mathcal{B}\|_0 \leq s \right\}, \quad (18)$$

which implies that the underlying tensor has a nonnegative factorization with tensor-tensor product and one factor tensor is sparse. We only know the joint probability density function or probability mass function of observations \mathcal{Y}_Ω given by (1). Let $\tilde{\mathcal{X}}$ be an estimator of \mathcal{X}^* . The risk of estimators with incomplete observations is defined as

$$\mathfrak{R}_{\tilde{\mathcal{X}}} = \frac{\mathbb{E}_{\Omega, \mathcal{Y}_\Omega}[\|\tilde{\mathcal{X}} - \mathcal{X}^*\|_F^2]}{n_1 n_2 n_3}. \quad (19)$$

The worst-case performance of an estimator $\tilde{\mathcal{X}}$ over the set $\mathfrak{U}(r, k, c)$ is defined as

$$\inf_{\tilde{\mathcal{X}}} \sup_{\mathcal{X}^* \in \mathfrak{U}(r, b, s)} \mathfrak{R}_{\tilde{\mathcal{X}}}.$$

The estimator is defined to achieve the minimax risk when it is the smallest maximum risk among all possible estimators. Denote

$$\Delta := \min \left\{ 1, \frac{s}{n_2 n_3} \right\}. \quad (20)$$

Now we establish the lower bounds of the minimax risk, whose proof follows a similar line of [21, Theorem 1] for noisy matrix completion, see also [54, Theorem 3]. The main technique is to define suitable packing sets for two factor tensors \mathcal{A} and \mathcal{B} in (18) based on tensor-tensor product. Then we construct binary sets for the two packing sets in the tensor form, which are subsets of (18). The line is mainly on the general results for the risk estimate based on KL divergence [55, Theorem 2.5] and the measures of two probability distributions. In this case, we need to establish the lower bounds of Hamming distance between any two binary sequences based on Varshamov-Gilbert bound [55, Lemma 2.9].

First we establish the minimax lower bound with a general class of noise models in (1), whose joint probability density function or probability mass function of observations is given.

Theorem 5.1: Suppose that the KL divergence of the scalar probability density function or probability mass function satisfies

$$D(p(x)||q(x)) \leq \frac{1}{2\nu^2}(x - y)^2, \quad (21)$$

where $\nu > 0$ depends on the distribution of observations in (1). Assume that \mathcal{Y}_Ω follows from (1). Let $r \leq \min\{n_1, n_2\}$ and $r \leq s \leq rn_2 n_3$. Then there exist $C, \beta_c > 0$ such that the minimax risk in (19) satisfies

$$\inf_{\tilde{\mathcal{X}}} \sup_{\mathcal{X}^* \in \mathfrak{U}(r, b, s)} \frac{\mathbb{E}_{\Omega, \mathcal{Y}_\Omega} \|\tilde{\mathcal{X}} - \mathcal{X}^*\|_F^2}{n_1 n_2 n_3} \geq C \min \left\{ \Delta b^2, \beta_c^2 \nu^2 \left(\frac{s + rn_1 n_3}{m} \right) \right\},$$

where Δ is defined as (20).

From Theorem 5.1, we know that the minimax lower bound matches the upper error bound in Theorem 4.1 with a logarithmic factor $\log(n_1 \vee n_2)$, which implies that the upper error bound in Theorem 4.1 is nearly optimal up to a logarithmic factor $\log(n_1 \vee n_2)$.

Remark V.1: For the minimax lower bound with general noise observations in Theorem 5.1, the main differences of proofs between [21] and Theorem 5.1 are the constructions of packing sets (the sets in (51), (52), (53)) for the set $\mathfrak{U}(r, b, s)$ in (18), where the tensor-tensor product is used in the set (51). Moreover, being different from the proof of [21], we need to construct the subsets of the packing sets (the sets in (54) and (59)), where the tensor in the subsets has special nonnegative tensor factorization structures with the tensor-tensor product form. The special block tensors are constructed for one factor tensor and special sets with block structure tensors are constructed for the other factor tensor (see (55) and (60)).

In the next subsections, we establish the explicit lower bounds for the special noise distributions, including additive Gaussian noise, additive Laplace noise, and Poisson observations, where the condition (21) can be satisfied easily in each case.

A. Additive Gaussian Noise

In this subsection, we establish the minimax lower bound for the observations with additive Gaussian noise, i.e., \mathcal{Y}_Ω obeys to (7). By Theorem 5.1, the key issue is to give the explicit ν in (21).

Proposition 5.1: Assume that \mathcal{Y}_Ω follows from (7). Let $r \leq \min\{n_1, n_2\}$ and $r \leq s \leq rn_2n_3$. Then there exist $C, \beta_c > 0$ such that the minimax risk in (19) satisfies

$$\inf_{\tilde{\mathcal{X}}} \sup_{\mathcal{X}^* \in \mathcal{U}(r, b, s)} \frac{\mathbb{E}_{\Omega, \mathcal{Y}_\Omega} \|\tilde{\mathcal{X}} - \mathcal{X}^*\|_F^2}{n_1 n_2 n_3} \geq C \min \left\{ \Delta b^2, \beta_c^2 \sigma^2 \left(\frac{s + rn_1 n_3}{m} \right) \right\},$$

where Δ is defined as (20).

Remark V.2: From Proposition 5.1, we know that the minmax lower bound matches the upper error bound in Proposition 4.1 with a logarithmic factor $\log(n_1 \vee n_2)$, which implies that the upper error bound in Proposition 4.1 is nearly optimal.

Remark V.3: When we observe all entries of \mathcal{Y} , i.e., $m = n_1 n_2 n_3$, Proposition 5.1 is just the minimax lower bound of sparse NTF with tensor-tensor product, which has been applied in dictionary learning [46].

B. Additive Laplace Noise

In this subsection, we establish the minimax lower bound for the observations with additive Laplace noise, i.e., \mathcal{Y}_Ω obeys to (11). Similar to the case of additive Gaussian noise, we only need to give ν in (21) in Theorem 5.1.

Proposition 5.2: Assume that \mathcal{Y}_Ω follows from (11). Let $r \leq \min\{n_1, n_2\}$ and $r \leq s \leq rn_2n_3$. Then there exist $C, \beta_c > 0$ such that the minimax risk in (19) satisfies

$$\inf_{\tilde{\mathcal{X}}} \sup_{\mathcal{X}^* \in \mathcal{U}(r, b, s)} \frac{\mathbb{E}_{\Omega, \mathcal{Y}_\Omega} \|\tilde{\mathcal{X}} - \mathcal{X}^*\|_F^2}{n_1 n_2 n_3} \geq C \min \left\{ \Delta b^2, \beta_c^2 \tau^2 \left(\frac{s + rn_1 n_3}{m} \right) \right\}.$$

Remark V.4: It follows from Proposition 5.2 that the rate attained by our estimator in Proposition 4.2 is optimal up to a logarithmic factor $\log(n_1 \vee n_2)$, which is similar to the case of observations with additive Gaussian noise.

C. Poisson Observations

In this subsection, we establish the minimax lower bound for Poisson observations, i.e., \mathcal{Y}_Ω obeys to (14). There is a slight difference compared with additive Gaussian noise and Laplace noise, we need to assume that all entries of the underlying tensor are strictly positive, i.e., $\zeta := \min_{i,j,k} \mathcal{X}_{ijk}^* > 0$. Suppose that $\zeta < b$. Being different from the candidate set (18), each entry of the candidate tensor is also strictly positive. The candidate set is defined as follows:

$$\begin{aligned} \tilde{\mathcal{U}}(r, b, s, \zeta) := \left\{ \mathcal{X} = \mathcal{A} \diamond \mathcal{B} \in \mathbb{R}_+^{n_1 \times n_2 \times n_3} : \mathcal{X}_{ijk} \geq \zeta, \mathcal{A} \in \mathbb{R}_+^{n_1 \times r \times n_3}, 0 \leq \mathcal{A}_{ijk} \leq 1, \right. \\ \left. \mathcal{B} \in \mathbb{R}_+^{r \times n_2 \times n_3}, 0 \leq \mathcal{B}_{ijk} \leq b, \|\mathcal{B}\|_0 \leq s \right\}. \end{aligned} \quad (22)$$

Then we know that $\tilde{\mathcal{U}}(r, b, s, \zeta) \subseteq \mathcal{U}(r, b, s)$.

Now the lower bound of candidate estimators for Poisson observations is given in the following proposition, whose proof follows a similar line of the matrix case in [21, Theorem 6]. For the sake of completeness, we give it here. Similar to Theorem 5.1, the main differences between the matrix- and tensor-based methods are the packing sets for the two nonnegative factorization factors \mathcal{A} and \mathcal{B} . We mainly use the results in [55, Theorem 2.5] for the constructed packing sets and the Varshamov-Gilbert bound [55, Lemma 2.9] for the binary sets.

Proposition 5.3: Suppose that \mathcal{Y}_Ω follows from (14). Let $r \leq \min\{n_1, n_2\}$ and $n_2 n_3 < s \leq r n_2 n_3$. Then there exist $0 < \tilde{\beta}_c < 1$ and $\tilde{C} > 0$ such that

$$\inf_{\tilde{X}} \sup_{\mathcal{X}^* \in \tilde{\mathcal{U}}(r, b, s, \zeta)} \frac{\mathbb{E}_{\Omega, \mathcal{Y}_\Omega} \|\tilde{\mathcal{X}} - \mathcal{X}^*\|_F^2}{n_1 n_2 n_3} \geq \tilde{C} \min \left\{ \tilde{\Delta} b^2, \tilde{\beta}_c^2 \zeta \left(\frac{s - n_2 n_3 + r n_1 n_3}{m} \right) \right\},$$

where $\tilde{\Delta} := \min\{(1 - \varsigma)^2, \Delta_1\}$ with $\varsigma := \frac{\zeta}{b}$ and $\Delta_1 := \min\{1, \frac{s - n_2 n_3}{n_2 n_3}\}$.

Remark V.5: From Proposition 5.3, we note that the lower bound of Poisson observations is of the order $O(\frac{s - n_2 n_3 + r n_1 n_3}{m})$. In particular, when $s \geq 2n_2 n_3$, the lower bound in Proposition 5.3 matches the upper bound in Proposition 4.3 up to a logarithmic factor $\log(n_1 \vee n_2)$.

Remark V.6: For the minimax lower bound with Poisson observations in Proposition 5.3, the main differences of proofs between [21] and Proposition 5.3 are the constructions of packing sets (the sets in (63), (64), (65)) for the set $\tilde{\mathcal{U}}(r, b, s, \zeta)$ in (22), where the tensor-tensor product is used in the set (63). Moreover, the subsets of the packing sets with two nonnegative factor tensors (the sets in (66) and (70)) need to be constructed, where the tensor-tensor product is also used in the two subsets. Besides, in the two subsets, the special block tensors for one factor tensor and special sets with block tensors for the other factor tensor (see the sets in (67) and (71)) are constructed.

VI. OPTIMIZATION ALGORITHM

In this section, we present an ADMM based algorithm [47, 48] to solve the model (2). Note that the feasible set Γ in (3) is discrete which makes the algorithm design difficult. In order to use continuous optimization techniques, the discrete assumption of Γ is dropped. This may be justified by choosing a very large value of ϑ and by noting that continuous optimization algorithms use finite precision arithmetic when executed on a computer. Now we consider to solve the following relaxation model:

$$\begin{aligned} \min_{\mathcal{X}, \mathcal{A}, \mathcal{B}} \quad & -\log p_{\mathcal{X}_\Omega}(\mathcal{Y}_\Omega) + \lambda \|\mathcal{B}\|_0, \\ \text{s.t.} \quad & \mathcal{X} = \mathcal{A} \diamond \mathcal{B}, \quad 0 \leq \mathcal{X}_{ijk} \leq c, \quad 0 \leq \mathcal{A}_{ijk} \leq 1, \quad 0 \leq \mathcal{B}_{ijk} \leq b. \end{aligned} \quad (23)$$

Let $\mathcal{X}' = \{\mathcal{X} \in \mathbb{R}_+^{n_1 \times n_2 \times n_3} : 0 \leq \mathcal{X}_{ijk} \leq c\}$, $\mathcal{A} = \{\mathcal{A} \in \mathbb{R}_+^{n_1 \times r \times n_3} : 0 \leq \mathcal{A}_{ijk} \leq 1\}$, $\mathcal{B}' = \{\mathcal{B} \in \mathbb{R}_+^{r \times n_2 \times n_3} : 0 \leq \mathcal{B}_{ijk} \leq b\}$, and $\mathcal{Q} = \mathcal{X}, \mathcal{M} = \mathcal{A}, \mathcal{N} = \mathcal{B}, \mathcal{Z} = \mathcal{B}$. Then problem (23) can be rewritten equivalently as

$$\begin{aligned} \min_{\mathcal{X}, \mathcal{A}, \mathcal{B}, \mathcal{Q}, \mathcal{M}, \mathcal{N}, \mathcal{Z}} \quad & -\log p_{\mathcal{X}_\Omega}(\mathcal{Y}_\Omega) + \lambda \|\mathcal{N}\|_0 + \delta_{\mathcal{X}'}(\mathcal{Q}) + \delta_{\mathcal{A}}(\mathcal{M}) + \delta_{\mathcal{B}'}(\mathcal{Z}), \\ \text{s.t.} \quad & \mathcal{X} = \mathcal{A} \diamond \mathcal{B}, \quad \mathcal{Q} = \mathcal{X}, \quad \mathcal{M} = \mathcal{A}, \quad \mathcal{N} = \mathcal{B}, \quad \mathcal{Z} = \mathcal{B}, \end{aligned} \quad (24)$$

where $\delta_{\mathcal{A}}(x)$ denotes the indicator function of \mathcal{A} , i.e., $\delta_{\mathcal{A}}(x) = 0$ if $x \in \mathcal{A}$ otherwise ∞ . The augmented Lagrangian function associated with (24) is defined as

$$\begin{aligned} & L(\mathcal{X}, \mathcal{A}, \mathcal{B}, \mathcal{Q}, \mathcal{M}, \mathcal{N}, \mathcal{Z}, \mathcal{T}_i) \\ & := -\log p_{\mathcal{X}_\Omega}(\mathcal{Y}_\Omega) + \lambda \|\mathcal{N}\|_0 + \delta_{\mathcal{X}'}(\mathcal{Q}) + \delta_{\mathcal{A}}(\mathcal{M}) + \delta_{\mathcal{B}'}(\mathcal{Z}) - \langle \mathcal{T}_1, \mathcal{X} - \mathcal{A} \diamond \mathcal{B} \rangle \\ & \quad - \langle \mathcal{T}_2, \mathcal{Q} - \mathcal{X} \rangle - \langle \mathcal{T}_3, \mathcal{M} - \mathcal{A} \rangle - \langle \mathcal{T}_4, \mathcal{N} - \mathcal{B} \rangle - \langle \mathcal{T}_5, \mathcal{Z} - \mathcal{B} \rangle \\ & \quad + \frac{\rho}{2} \left(\|\mathcal{X} - \mathcal{A} \diamond \mathcal{B}\|_F^2 + \|\mathcal{Q} - \mathcal{X}\|_F^2 + \|\mathcal{M} - \mathcal{A}\|_F^2 + \|\mathcal{N} - \mathcal{B}\|_F^2 + \|\mathcal{Z} - \mathcal{B}\|_F^2 \right), \end{aligned}$$

where \mathcal{T}_i are Lagrangian multipliers, $i = 1, \dots, 5$, and $\rho > 0$ is the penalty parameter. The iteration of ADMM is given as follows:

$$\begin{aligned}\mathcal{X}^{k+1} &= \arg \min_{\mathcal{X}} L(\mathcal{X}, \mathcal{A}^k, \mathcal{B}^k, \mathcal{Q}^k, \mathcal{M}^k, \mathcal{N}^k, \mathcal{Z}^k, \mathcal{T}_i^k) \\ &= \text{Prox}_{(-\frac{1}{2\rho} \log p_{\mathcal{X}\Omega}(\mathcal{Y}_\Omega))} \left(\frac{1}{2} \left(\mathcal{Q}^k + \mathcal{A}^k \diamond \mathcal{B}^k + \frac{1}{\rho} (\mathcal{T}_1^k - \mathcal{T}_2^k) \right) \right),\end{aligned}\quad (25)$$

$$\begin{aligned}\mathcal{A}^{k+1} &= \arg \min_{\mathcal{A}} L(\mathcal{X}^{k+1}, \mathcal{A}, \mathcal{B}^k, \mathcal{Q}^k, \mathcal{M}^k, \mathcal{N}^k, \mathcal{Z}^k, \mathcal{T}_i^k) \\ &= \left(\mathcal{M}^k + (\mathcal{X}^{k+1} - \frac{1}{\rho} \mathcal{T}_1^k) \diamond (\mathcal{B}^k)^T - \frac{1}{\rho} \mathcal{T}_3^k \right) \diamond (\mathcal{B}^k \diamond (\mathcal{B}^k)^T + \mathcal{I})^{-1},\end{aligned}\quad (26)$$

$$\begin{aligned}\mathcal{B}^{k+1} &= \arg \min_{\mathcal{B}} L(\mathcal{X}^{k+1}, \mathcal{A}^{k+1}, \mathcal{B}, \mathcal{Q}^k, \mathcal{M}^k, \mathcal{N}^k, \mathcal{Z}^k, \mathcal{T}_i^k) \\ &= ((\mathcal{A}^{k+1})^T \diamond \mathcal{A}^{k+1} + 2\mathcal{I})^{-1} \diamond \\ &\quad \left((\mathcal{A}^{k+1})^T \diamond \mathcal{X}^{k+1} + \mathcal{N}^k + \mathcal{Z}^k - \frac{1}{\rho} ((\mathcal{A}^{k+1})^T \diamond \mathcal{T}_1^k + \mathcal{T}_4^k + \mathcal{T}_5^k) \right),\end{aligned}\quad (27)$$

$$\mathcal{Q}^{k+1} = \arg \min_{\mathcal{Q}} L(\mathcal{X}^{k+1}, \mathcal{A}^{k+1}, \mathcal{B}^{k+1}, \mathcal{Q}, \mathcal{M}^k, \mathcal{N}^k, \mathcal{Z}^k, \mathcal{T}_i^k) = \Pi_{\mathcal{X}'} \left(\mathcal{X}^{k+1} + \frac{1}{\rho} \mathcal{T}_2^k \right), \quad (28)$$

$$\mathcal{M}^{k+1} = \arg \min_{\mathcal{M}} L(\mathcal{X}^{k+1}, \mathcal{A}^{k+1}, \mathcal{B}^{k+1}, \mathcal{Q}^{k+1}, \mathcal{M}, \mathcal{N}^k, \mathcal{Z}^{k+1}, \mathcal{T}_i^k) = \Pi_{\mathcal{A}} \left(\mathcal{A}^{k+1} + \frac{1}{\rho} \mathcal{T}_3^k \right), \quad (29)$$

$$\begin{aligned}\mathcal{N}^{k+1} &= \arg \min_{\mathcal{N}} L(\mathcal{X}^{k+1}, \mathcal{A}^{k+1}, \mathcal{B}^{k+1}, \mathcal{Q}^{k+1}, \mathcal{M}^{k+1}, \mathcal{N}, \mathcal{Z}^k, \mathcal{T}_i^k) \\ &= \text{Prox}_{\frac{\lambda}{\rho} \|\cdot\|_0} \left(\mathcal{B}^{k+1} + \frac{1}{\rho} \mathcal{T}_4^k \right),\end{aligned}\quad (30)$$

$$\mathcal{Z}^{k+1} = \arg \min_{\mathcal{Z}} L(\mathcal{X}^{k+1}, \mathcal{A}^{k+1}, \mathcal{B}^{k+1}, \mathcal{Q}^{k+1}, \mathcal{M}^{k+1}, \mathcal{N}^{k+1}, \mathcal{Z}, \mathcal{T}_i^k) = \Pi_{\mathcal{B}'} \left(\mathcal{B}^{k+1} + \frac{1}{\rho} \mathcal{T}_5^k \right), \quad (31)$$

$$\mathcal{T}_1^{k+1} = \mathcal{T}_1^k - \rho(\mathcal{X}^{k+1} - \mathcal{A}^{k+1} \diamond \mathcal{B}^{k+1}), \quad \mathcal{T}_2^{k+1} = \mathcal{T}_2^k - \rho(\mathcal{Q}^{k+1} - \mathcal{X}^{k+1}), \quad (32)$$

$$\mathcal{T}_3^{k+1} = \mathcal{T}_3^k - \rho(\mathcal{M}^{k+1} - \mathcal{A}^{k+1}), \quad \mathcal{T}_4^{k+1} = \mathcal{T}_4^k - \rho(\mathcal{N}^{k+1} - \mathcal{B}^{k+1}), \quad (33)$$

$$\mathcal{T}_5^{k+1} = \mathcal{T}_5^k - \rho(\mathcal{Z}^{k+1} - \mathcal{B}^{k+1}), \quad (34)$$

where $\Pi_{\mathcal{X}'}(\mathcal{X})$, $\Pi_{\mathcal{A}}(\mathcal{X})$, and $\Pi_{\mathcal{B}'}(\mathcal{X})$ denote the projections of \mathcal{X} onto the sets \mathcal{X}' , \mathcal{A} , and \mathcal{B}' , respectively.

Now the ADMM for solving (24) is stated in Algorithm 1.

Algorithm 1 Alternating Direction Method of Multipliers for Solving (24)

Input. Let $\rho > 0$ be a given constant. Given $\mathcal{A}^0, \mathcal{B}^0, \mathcal{Q}^0, \mathcal{M}^0, \mathcal{N}^0, \mathcal{Z}^0, \mathcal{T}_i^0, i = 1, \dots, 5$. For $k = 0, 1, \dots$, perform the following steps:

Step 1. Compute \mathcal{X}^{k+1} via (25).

Step 2. Compute \mathcal{A}^{k+1} by (26).

Step 3. Compute \mathcal{B}^{k+1} by (27).

Step 4. Compute $\mathcal{Q}^{k+1}, \mathcal{M}^{k+1}, \mathcal{N}^{k+1}, \mathcal{Z}^{k+1}$ by (28), (29), (30), and (31), respectively.

Step 5. Update $\mathcal{T}_1^{k+1}, \mathcal{T}_2^{k+1}, \mathcal{T}_3^{k+1}, \mathcal{T}_4^{k+1}, \mathcal{T}_5^{k+1}$ via (32), (33), and (34), respectively.

Step 6. If a termination criterion is not satisfied, set $k := k + 1$ and go to Step 1.

Algorithm 1 is an ADMM based algorithm for solving nonconvex optimization problems. Although great efforts have been made about the convergence of ADMM for nonconvex models in recent years [48, 56], the existing ADMM based algorithm cannot be applied to our model directly since both the objective function and constraints are nonconvex. Moreover, the data-fitting term is nonsmooth when the observations are corrupted by additive Laplace noise, which also gives rise to the difficulty of the convergence of ADMM for solving our model.

Remark VI.1: In Algorithm 1, one needs to compute the proximal mapping $\text{Prox}_{(-\frac{1}{2\rho} \log p_{\mathcal{X}_\Omega}(\mathcal{Y}_\Omega))}(\mathcal{S})$, where $\mathcal{S} = \frac{1}{2}(\mathcal{Q}^k + \mathcal{A}^k \diamond \mathcal{B}^k + \frac{1}{\rho}(\mathcal{T}_1^k - \mathcal{T}_2^k))$. In particular, for the additive Gaussian noise, additive Laplace noise, and Poisson observations, the proximal mappings at \mathcal{S} are given by

- Additive Gaussian noise:

$$\text{Prox}_{(-\frac{1}{2\rho} \log p_{\mathcal{X}_\Omega}(\mathcal{Y}_\Omega))}(\mathcal{S}) = \mathcal{P}_\Omega \left(\frac{\mathcal{Y} + 2\rho\sigma^2\mathcal{S}}{1 + 2\rho\sigma^2} \right) + \mathcal{P}_{\bar{\Omega}}(\mathcal{S}),$$

where $\bar{\Omega}$ is the complementary set of Ω .

- Additive Laplace noise:

$$\text{Prox}_{(-\frac{1}{2\rho} \log p_{\mathcal{X}_\Omega}(\mathcal{Y}_\Omega))}(\mathcal{S}) = \mathcal{P}_\Omega \left(\mathcal{Y}_\Omega + \text{sign}(\mathcal{S} - \mathcal{Y}_\Omega) \circ \max \left\{ |\mathcal{S} - \mathcal{Y}_\Omega| - \frac{1}{2\rho\tau}, 0 \right\} \right) + \mathcal{P}_{\bar{\Omega}}(\mathcal{S}),$$

where $\text{sign}(\cdot)$ denotes the signum function and \circ denotes the point-wise product.

- Poisson observations:

$$\text{Prox}_{(-\frac{1}{2\rho} \log p_{\mathcal{X}_\Omega}(\mathcal{Y}_\Omega))}(\mathcal{S}) = \mathcal{P}_\Omega \left(\frac{2\rho\mathcal{S} - \mathbb{I} + \sqrt{(2\rho\mathcal{S} - \mathbb{I})^2 + 8\rho\mathcal{Y}}}{4\rho} \right) + \mathcal{P}_{\bar{\Omega}}(\mathcal{S}),$$

where $\mathbb{I} \in \mathbb{R}^{n_1 \times r \times n_3}$ denotes the tensor with all entries being 1, and the square and root are performed in point-wise manners.

Remark VI.2: We also need to compute the proximal mapping of tensor ℓ_0 norm [57] in Algorithm 1. Note that the tensor ℓ_0 norm is separable. Then we just need to derive its scalar form. For any $t > 0$, the proximal mapping of $t\|\cdot\|_0$ is given by (see, e.g., [58, Example 6.10])

$$\text{Prox}_{t\|\cdot\|_0}(y) = \begin{cases} 0, & \text{if } |y| < \sqrt{2t}, \\ \{0, y\}, & \text{if } |y| = \sqrt{2t}, \\ y, & \text{if } |y| > \sqrt{2t}. \end{cases}$$

Remark VI.3: The ADMM based algorithm is developed to solve the model (24). However, the problem (24) is nonconvex, and it is difficult to obtain its global optimal solution in experiments, while the estimators of the upper error bounds in Section IV are globally optimal.

Remark VI.4: The main cost of ADMM in Algorithm 1 is the tensor-tensor product and tensor inverse operations. First, we consider the computational cost of the tensor-tensor product for two tensors $\mathcal{A} \in \mathbb{R}^{n_1 \times r \times n_3}$ and $\mathcal{B} \in \mathbb{R}^{r \times n_2 \times n_3}$, which is implemented by fast Fourier transform [33]. The application of discrete Fourier transform to an n_3 -vector is of $O(n_3 \log(n_3))$ operations. After Fourier transform along the tubes, we need to compute n_3 matrix products with sizes n_1 -by- r and r -by- n_2 , whose cost is $O(rn_1n_2n_3)$. Therefore, for the tensor-tensor product of $\mathcal{A} \in \mathbb{R}^{n_1 \times r \times n_3}$ and $\mathcal{B} \in \mathbb{R}^{r \times n_2 \times n_3}$, the total cost is $O(r(n_1 + n_2)n_3 \log(n_3) + rn_1n_2n_3)$. Second, for the inverse operation of an $n \times n \times n_3$ tensor, one takes fast Fourier transform along the third-dimension and operates the inverse for each frontal slice in the Fourier domain. Then the total cost of the tensor inverse is $O(n^2n_3 \log(n_3) + n^3n_3)$. For the ADMM, its main cost is to compute \mathcal{A}^{k+1} and \mathcal{B}^{k+1} . The complexities of computing \mathcal{A}^{k+1} and \mathcal{B}^{k+1} are $O(n_2(r + n_1)n_3 \log(n_3) +$

$rn_1n_2n_3$) and $O(n_1(r + n_2)n_3 \log(n_3) + rn_1n_2n_3)$, respectively. Note that $r \leq \min\{n_1, n_2\}$. If we take one of the proximal mappings in Remark VI.1 for \mathcal{X}^{k+1} , the total cost of ADMM is $O(n_1n_2n_3 \log(n_3) + rn_1n_2n_3)$.

VII. NUMERICAL RESULTS

In this section, some numerical experiments are conducted to demonstrate the effectiveness of the proposed tensor-based method for sparse NTF and completion with different noise observations, including additive Gaussian noise, additive Laplace noise, and Poisson observations. We will compare the sparse NTF and completion method with the matrix-based method in [20].

The Karush-Kuhn-Tucker (KKT) conditions of (24) are given by

$$\begin{cases} 0 \in \partial_{\mathcal{X}}(-\log(p_{\mathcal{X}_\Omega}(\mathcal{Y}_\Omega))) - \mathcal{T}_1 + \mathcal{T}_2, \\ \mathcal{T}_1 \diamond \mathcal{B}^T + \mathcal{T}_3 = 0, \mathcal{A}^T \diamond \mathcal{T}_1 + \mathcal{T}_4 + \mathcal{T}_5 = 0, \\ 0 \in \partial_{\mathcal{X}'}(\mathcal{Q}) - \mathcal{T}_2, 0 \in \partial_{\mathcal{M}}(\mathcal{M}) - \mathcal{T}_3, \\ 0 \in \partial(\lambda \|\mathcal{N}\|_0) - \mathcal{T}_4, 0 \in \partial_{\mathcal{B}'}(\mathcal{Z}) - \mathcal{T}_5, \\ \mathcal{X} = \mathcal{A} \diamond \mathcal{B}, \mathcal{Q} = \mathcal{X}, \mathcal{M} = \mathcal{A}, \mathcal{N} = \mathcal{B}, \mathcal{Z} = \mathcal{B}, \end{cases} \quad (35)$$

where $\partial f(x)$ denotes the subdifferential of f at x . Based on the KKT conditions in (35), we adopt the following relative residual to measure the accuracy:

$$\eta_{max} := \max\{\eta_1, \eta_2, \eta_3, \eta_4, \eta_5, \eta_6\},$$

where

$$\begin{aligned} \eta_1 &= \frac{\|\mathcal{X} - \text{Prox}_{(-\log(p_{\mathcal{X}_\Omega}(\mathcal{Y}_\Omega)))}(\mathcal{T}_1 - \mathcal{T}_2 + \mathcal{X})\|_F}{1 + \|\mathcal{X}\|_F + \|\mathcal{T}_1\|_F + \|\mathcal{T}_2\|_F}, \quad \eta_2 = \frac{\|\mathcal{Q} - \Pi_{\mathcal{X}'}(\mathcal{T}_2 + \mathcal{Q})\|_F}{1 + \|\mathcal{T}_2\|_F + \|\mathcal{Q}\|_F}, \\ \eta_3 &= \frac{\|\mathcal{M} - \Pi_{\mathcal{M}}(\mathcal{T}_3 + \mathcal{M})\|_F}{1 + \|\mathcal{T}_3\|_F + \|\mathcal{M}\|_F}, \quad \eta_4 = \frac{\|\mathcal{N} - \text{Prox}_{\lambda \|\cdot\|_0}(\mathcal{T}_4 + \mathcal{N})\|_F}{1 + \|\mathcal{T}_4\|_F + \|\mathcal{N}\|_F}, \\ \eta_5 &= \frac{\|\mathcal{Z} - \Pi_{\mathcal{B}'}(\mathcal{T}_5 + \mathcal{Z})\|_F}{1 + \|\mathcal{T}_5\|_F + \|\mathcal{Z}\|_F}, \quad \eta_6 = \frac{\|\mathcal{X} - \mathcal{A} \diamond \mathcal{B}\|_F}{1 + \|\mathcal{X}\|_F + \|\mathcal{A}\|_F + \|\mathcal{B}\|_F}. \end{aligned}$$

Algorithm 1 is terminated if $\eta_{max} \leq 10^{-4}$ or the number of iterations reaches the maximum of 300.

In order to measure the quality of the recovered tensor, the relative error (RE) is used to evaluate the performance of different methods, which is defined as

$$\text{RE} = \frac{\|\tilde{\mathcal{X}} - \mathcal{X}^*\|_F}{\|\mathcal{X}^*\|_F},$$

where $\tilde{\mathcal{X}}$ and \mathcal{X}^* are the recovered tensor and the ground-truth tensor, respectively.

We generate the nonnegative tensors $\mathcal{A}^* \in \mathbb{R}_+^{n_1 \times r \times n_3}$ and $\mathcal{B}^* \in \mathbb{R}_+^{r \times n_2 \times n_3}$ at random. \mathcal{A}^* is generated by the MATLAB command `rand(n1, r, n3)` and \mathcal{B}^* is a nonnegative sparse tensor generated by the tensor toolbox command `b · sptenrand([r, n2, n3], s)` [59], where b is the magnitude of \mathcal{B}^* and s is the sparse ratio. Then $\mathcal{X}^* = \mathcal{A}^* \diamond \mathcal{B}^*$ and we choose $c = 2\|\mathcal{X}^*\|_\infty$. The size of the testing third-order tensors is $n_1 = n_2 = n_3 = 100$ in the following two experiments. The initial values will also influence the performance of ADMM. For the initial values $\mathcal{A}^0, \mathcal{B}^0, \mathcal{M}^0, \mathcal{N}^0, \mathcal{Z}^0, \mathcal{T}_3^0, \mathcal{T}_4^0, \mathcal{T}_5^0$ of ADMM, we choose them as two random tensors with the same size as that of $\mathcal{A}^*, \mathcal{B}^*$. For the initial values $\mathcal{Q}^0, \mathcal{T}_1^0, \mathcal{T}_2^0$, we choose them as the observations \mathcal{Y}_Ω in Ω and zeros outside Ω .

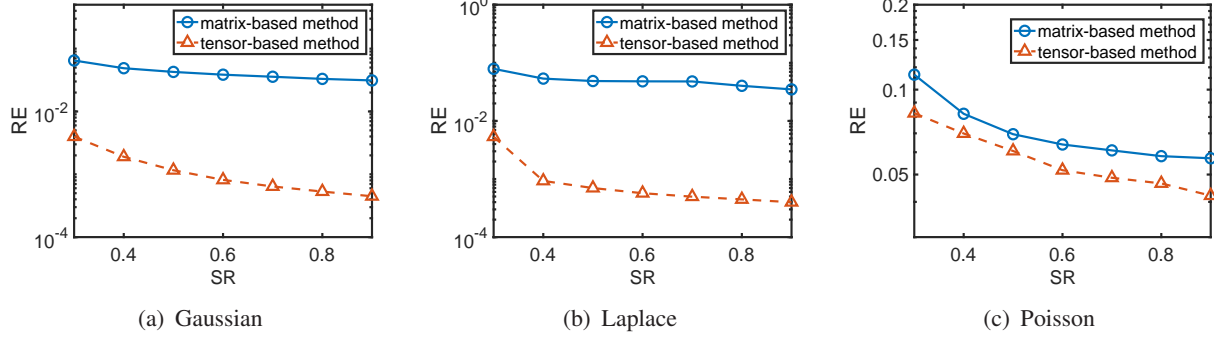


Fig. 1: RE versus SR of different methods for different noise observations. (a) Gaussian. (b) Laplace. (c) Poisson.

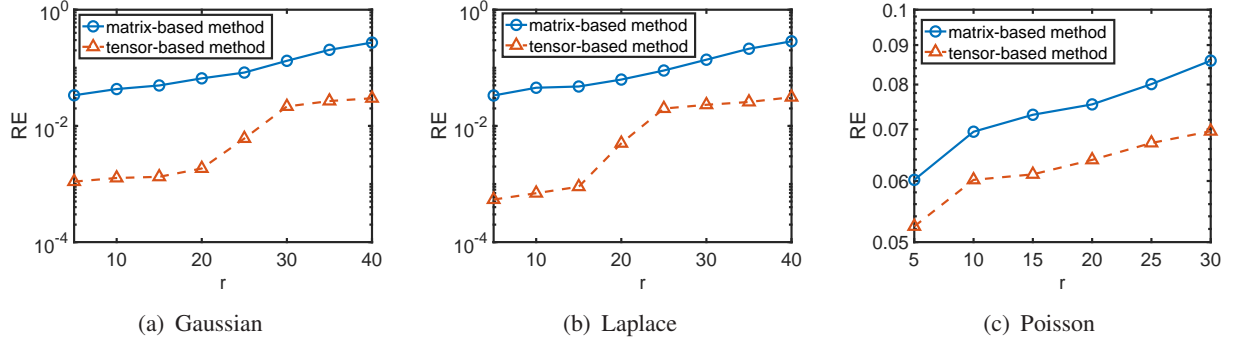


Fig. 2: RE versus r of different methods for different noise observations. (a) Gaussian. (b) Laplace. (c) Poisson.

As discussed in Section III, we aim to estimate the ground-truth tensor \mathcal{X}^* . Note that the two factors may not be unique. Therefore, we only compare the recovered tensor $\tilde{\mathcal{X}}$ with the ground-truth tensor \mathcal{X}^* in the experiments. In fact, we just establish the error upper bounds of \mathcal{X} , and do not analyze the error bounds of each factor tensor independently in theory.

First we analyze the recovery performance of different methods versus SRs. In Figure 1, we display the REs of the recovered tensors with different sampling ratios and r , where the sparse ratio $s = 0.3$ and the observed entries are corrupted by Gaussian noise, Laplace noise, and Poisson noise, respectively. We set $\sigma = 0.1$ and $\tau = 0.1$ for Gaussian noise and Laplace noise, respectively, and $r = 10$ and $b = 2$. The SRs vary from 0.3 to 0.9 with step size 0.1. It can be seen from this figure that the relative errors decrease when the sampling ratios increase for both matrix- and tensor-based methods. Moreover, the relative errors obtained by the tensor-based method are lower than those obtained by the matrix-based method. Compared with the matrix-based method, the improvements of the tensor-based method for additive Gaussian noise and Laplace noise are much more than those for Poisson observations, where the main reason is that the constants of the upper bound in Proposition 4.3 are slightly larger than those of the matrix-based method in [20] for Poisson observations.

The recovery performance of different methods versus r is also analyzed, where $\text{SR} = 0.5$ and r varies from 5 to 40 with step size 5 for additive Gaussian noise and Laplace noise, and from 5 to 30 with step size 5 for Poisson observations. Again we set $b = 2$, and $\sigma = 0.1$ and $\tau = 0.1$ for Gaussian noise and Laplace noise, respectively. It can be seen from Figure 2 that

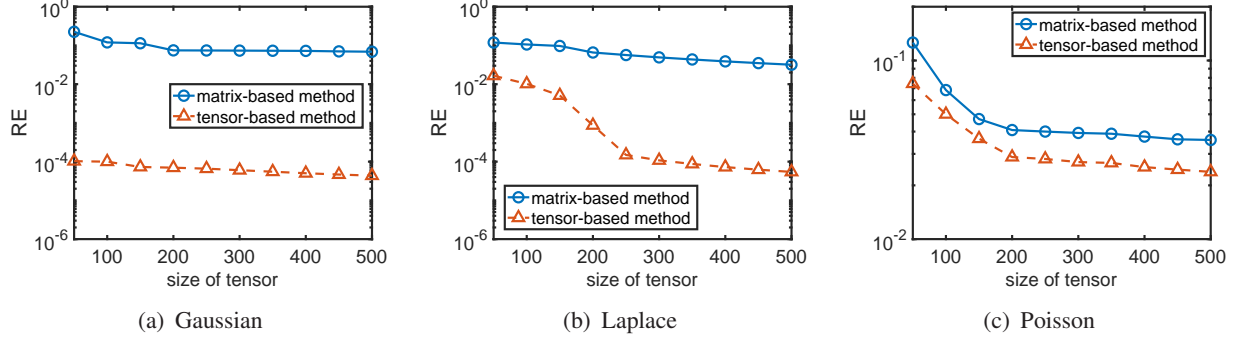


Fig. 3: RE versus size of tensors of different methods for different noise observations. (a) Gaussian. (b) Laplace. (c) Poisson.

the relative errors obtained by the tensor-based method are lower than those obtained by the matrix-based method for the three noise models. Besides, we can observe that REs increase when r increases for both matrix- and tensor-based methods. Again the tensor-based method performs better than the matrix-based method for different r and noise observations. Compared with Poisson observations, the improvements of the tensor-based method are much more for the additive Gaussian noise and Laplace noise.

In Figure 3, we test different sizes $n := n_1 = n_2 = n_3$ of tensors, and vary n from 50 to 500 with step size 50, where $\text{SR} = 0.5$, the sparse ratio $s = 0.3$, $r = 10$, and $b = 2$. Here we set $\sigma = 0.1$ for Gaussian noise and $\tau = 0.1$ for Laplace noise, respectively. It can be observed from this figure that the relative errors of the tensor-based method are smaller than those of the matrix-based method for different noise distributions. The relative errors of both matrix- and tensor-based methods decrease as n increases. Furthermore, for different size n of the testing tensors, the improvements of relative errors of the tensor-based method for Gaussian noise and Laplace noise are much more than those for Poisson observations.

VIII. CONCLUDING REMARKS

In this paper, we have studied the sparse NTF and completion problem based on tensor-tensor product from partial and noisy observations, where the observations are corrupted by general noise distributions. A maximum likelihood estimate of partial observations is derived for the data-fitting term and the tensor ℓ_0 norm is adopted to enforce the sparsity of the sparse factor. Then an upper error bound is established for a general class of noise models, and is specialized to widely used noise distributions including additive Gaussian noise, additive Laplace noise, and Poisson observations. Moreover, the minimax lower bounds are also established for the previous noise models, which match the upper error bounds up to logarithmic factors. An ADMM based algorithm is developed to solve the resulting model. Preliminary numerical experiments are presented to demonstrate the superior performance of the proposed tensor-based model compared with the matrix-based method [20].

It would be of great interest to study the upper error bounds of the convexification model by using the tensor ℓ_1 norm to replace the tensor ℓ_0 norm for the sparse factor. It would also be of great interest to establish the convergence of ADMM for our proposed model with general noise observations, which is nonconvex and has multi-block variables. Moreover, future work may extend the theory of sparse NTF and completion model with tensor-tensor product to that with

transformed tensor-tensor product under suitable unitary transformations [36], which is more effective than tensor-tensor product for robust tensor completion [36, 38] and data compression [60].

ACKNOWLEDGMENTS

The authors would like to thank the associate editor and anonymous referees for their helpful comments and constructive suggestions on improving the quality of this paper.

APPENDIX A

PROOF OF THEOREM 4.1

We begin by stating the following lemma which will be useful in the proof of Theorem 4.1.

Lemma A.1: Let Γ be a countable collection of candidate reconstructions \mathcal{X} of \mathcal{X}^* in (3) and its penalty $\text{pen}(\mathcal{X}) \geq 1$ satisfying $\sum_{\mathcal{X} \in \Gamma} 2^{-\text{pen}(\mathcal{X})} \leq 1$. For any integer $4 \leq m \leq n_1 n_2 n_3$, let $\Omega \sim \text{Bern}(\gamma)$. Moreover, the corresponding observations are obtained by $p_{\mathcal{X}^*}(\mathcal{Y}_\Omega) = \prod_{(i,j,k) \in \Omega} p_{\mathcal{X}_{ijk}^*}(\mathcal{Y}_{ijk})$, which are assumed to be conditionally independent given Ω . If

$$\kappa \geq \max_{\mathcal{X} \in \Gamma} \max_{i,j,k} D(p_{\mathcal{X}_{ijk}^*}(\mathcal{Y}_{ijk}) || p_{\mathcal{X}_{ijk}}(\mathcal{Y}_{ijk})), \quad (36)$$

then for any $\xi \geq 2 \left(1 + \frac{2\kappa}{3}\right) \log(2)$, the following penalized maximum likelihood estimator

$$\tilde{\mathcal{X}}^\xi \in \arg \min_{\mathcal{X} \in \Gamma} \{-\log p_{\mathcal{X}}(\mathcal{Y}_\Omega) + \xi \cdot \text{pen}(\mathcal{X})\}, \quad (37)$$

satisfies

$$\frac{\mathbb{E}_{\Omega, \mathcal{Y}_\Omega} [-2 \log H(p_{\tilde{\mathcal{X}}^\xi}, p_{\mathcal{X}^*})]}{n_1 n_2 n_3} \leq 3 \cdot \min_{\mathcal{X} \in \Gamma} \left\{ \frac{D(p_{\mathcal{X}^*} || p_{\mathcal{X}})}{n_1 n_2 n_3} + \left(\xi + \frac{4\kappa \log(2)}{3} \right) \frac{\text{pen}(\mathcal{X})}{m} \right\} + \frac{8\kappa \log(m)}{m},$$

where the expectation is taken with respect to the joint distribution of Ω and \mathcal{Y}_Ω .

The proof of Lemma A.1 can be derived easily based on the matrix case [20, Lemma 8], see also [61]. At its essence, the three steps of proof in [20, Lemma 8] are mainly in point-wise manners for the KL divergence, logarithmic Hellinger affinity, and maximum likelihood estimate. Therefore, we can extend them to the tensor case easily. For the sake of brevity, we omit the details here.

Next we give a lemma with respect to the upper bound of the tensor ℓ_∞ norm between a tensor and its closest surrogate in Γ .

Lemma A.2: Consider a candidate reconstruction of the form $\tilde{\mathcal{X}}^* = \tilde{\mathcal{A}}^* \diamond \tilde{\mathcal{B}}^*$, where each entry of $\tilde{\mathcal{A}}^* \in \mathfrak{L}$ is the closest discretized surrogates of the entries of \mathcal{A}^* , and each entry of $\tilde{\mathcal{B}}^* \in \mathfrak{D}$ is the closest discretized surrogates of the nonzero entries of \mathcal{B}^* , and zero otherwise. Then

$$\|\tilde{\mathcal{X}}^* - \mathcal{X}^*\|_\infty \leq \frac{3rn_3b}{\vartheta},$$

where ϑ is defined as (4).

Proof: Let $\tilde{\mathcal{A}}^* = \mathcal{A}^* + \Delta_{\mathcal{A}^*}$ and $\tilde{\mathcal{B}}^* = \mathcal{B}^* + \Delta_{\mathcal{B}^*}$. Then

$$\tilde{\mathcal{X}}^* - \mathcal{X}^* = \tilde{\mathcal{A}}^* \diamond \tilde{\mathcal{B}}^* - \mathcal{A}^* \diamond \mathcal{B}^* = \mathcal{A}^* \diamond \Delta_{\mathcal{B}^*} + \Delta_{\mathcal{A}^*} \diamond \mathcal{B}^* + \Delta_{\mathcal{A}^*} \diamond \Delta_{\mathcal{B}^*}.$$

By the definitions of $\tilde{\mathcal{A}}^*$ and $\tilde{\mathcal{B}}^*$, we know that

$$\|\Delta_{\mathcal{A}^*}\|_\infty \leq \frac{1}{\vartheta - 1} \quad \text{and} \quad \|\Delta_{\mathcal{B}^*}\|_\infty \leq \frac{b}{\vartheta - 1}. \quad (38)$$

By the definition of tensor-tensor product of two tensors, we deduce

$$\begin{aligned}\mathcal{A}^* \diamond \Delta_{\mathcal{B}^*} &= \text{Fold} \left(\text{Circ} \begin{pmatrix} (\mathbf{A}^*)^{(1)} \\ (\mathbf{A}^*)^{(2)} \\ \vdots \\ (\mathbf{A}^*)^{(n_3)} \end{pmatrix} \cdot \text{Unfold}(\Delta_{\mathcal{B}^*}) \right) \\ &= \text{Fold} \begin{pmatrix} (\mathbf{A}^*)^{(1)}(\Delta_{\mathcal{B}^*})^{(1)} + (\mathbf{A}^*)^{(n_3)}(\Delta_{\mathcal{B}^*})^{(2)} + \dots + (\mathbf{A}^*)^{(2)}(\Delta_{\mathcal{B}^*})^{(n_3)} \\ (\mathbf{A}^*)^{(2)}(\Delta_{\mathcal{B}^*})^{(1)} + (\mathbf{A}^*)^{(1)}(\Delta_{\mathcal{B}^*})^{(2)} + \dots + (\mathbf{A}^*)^{(3)}(\Delta_{\mathcal{B}^*})^{(n_3)} \\ \vdots \\ (\mathbf{A}^*)^{(n_3)}(\Delta_{\mathcal{B}^*})^{(1)} + (\mathbf{A}^*)^{(n_3-1)}(\Delta_{\mathcal{B}^*})^{(2)} + \dots + (\mathbf{A}^*)^{(1)}(\Delta_{\mathcal{B}^*})^{(n_3)} \end{pmatrix}.\end{aligned}$$

It follows from (38) and $0 \leq \mathcal{A}_{ijk}^* \leq 1$ that

$$\|\mathcal{A}^* \diamond \Delta_{\mathcal{B}^*}\|_\infty \leq n_3 \max_{i,j} \|(\mathbf{A}^*)^{(i)}(\Delta_{\mathcal{B}^*})^{(j)}\|_\infty \leq \frac{rn_3b}{\vartheta - 1}.$$

Similarly, we can get that $\|\Delta_{\mathcal{A}^*} \diamond \mathcal{B}^*\|_\infty \leq \frac{rn_3b}{\vartheta - 1}$ and $\|\Delta_{\mathcal{A}^*} \diamond \Delta_{\mathcal{B}^*}\|_\infty \leq \frac{rn_3b}{(\vartheta - 1)^2}$. Therefore, we obtain that

$$\begin{aligned}\|\tilde{\mathcal{A}}^* \diamond \tilde{\mathcal{B}}^* - \mathcal{A}^* \diamond \mathcal{B}^*\|_\infty &\leq \|\mathcal{A}^* \diamond \Delta_{\mathcal{B}^*}\|_\infty + \|\Delta_{\mathcal{A}^*} \diamond \mathcal{B}^*\|_\infty + \|\Delta_{\mathcal{A}^*} \diamond \Delta_{\mathcal{B}^*}\|_\infty \\ &\leq \frac{rn_3b}{\vartheta - 1} + \frac{rn_3b}{\vartheta - 1} + \frac{rn_3b}{(\vartheta - 1)^2} \\ &\leq \frac{3rn_3b}{\vartheta},\end{aligned}$$

where the last inequality holds by $\vartheta \geq 8$ in (4). The proof is completed. \blacksquare

Remark A.1: By the construction of $\tilde{\mathcal{B}}^*$ in Lemma A.2, we know that $\|\tilde{\mathcal{B}}^*\|_0 = \|\mathcal{B}^*\|_0$, which will be used to establish the upper bounds in the specifical noise models.

Now we return to prove Theorem 4.1. First, we need to define the penalty $\text{pen}(\mathcal{X})$ on the candidate reconstructions \mathcal{X} of \mathcal{X}^* in the set Γ such that the summability condition

$$\sum_{\mathcal{X} \in \Gamma} 2^{-\text{pen}(\mathcal{X})} \leq 1 \quad (39)$$

holds. Notice that the condition in (39) is the well-known Kraft-McMillan inequality for coding entries of Γ with an alphabet of size 2 [50, 51], see also [62, Section 5]. If we choose the penalties to be code lengths for some uniquely decodable binary code of the entries $\mathcal{X} \in \Gamma$, then (39) is satisfied automatically [62, Section 5], which will provide the construction of the penalties.

Next we consider the discretized tensor factors $\mathcal{A} \in \mathfrak{L}$ and $\mathcal{B} \in \mathfrak{D}$. Fix an ordering of the indices of entries of \mathcal{A} and encode the amplitude of each entry using $\log_2(\vartheta)$ bits. Let $\tilde{\vartheta} := 2^{\lceil \log_2(rn_2) \rceil}$. Similarly, we encode each nonzero entry of \mathcal{B} using $\log_2(\vartheta)$ bits to denote its location and $\log_2(\vartheta)$ bits for its amplitude. By this construction, a total of $rn_1n_3 \log_2(\vartheta)$ bits are used to encode \mathcal{A} . Note that \mathcal{B} has $\|\mathcal{B}\|_0$ nonzero entries. Then a total of $\|\mathcal{B}\|_0(\log_2(\tilde{\vartheta}) + \log_2(\vartheta))$ bits are used to encode \mathcal{B} . Therefore, we define the penalties $\text{pen}(\mathcal{X})$ to all $\mathcal{X} \in \Gamma$ as the encoding lengths, i.e.,

$$\text{pen}(\mathcal{X}) = rn_1n_3 \log_2(\vartheta) + \|\mathcal{B}\|_0(\log_2(\tilde{\vartheta}) + \log_2(\vartheta)).$$

By the above construction, it is easy to see that such codes are uniquely decodable. Thus, by Kraft-McMillan inequality [50, 51], we get that $\sum_{\mathcal{X} \in \Gamma} 2^{-\text{pen}(\mathcal{X})} \leq 1$.

Let $\lambda = \xi(\log_2(\vartheta) + \log_2(\tilde{\vartheta}))$, where ξ is the regularization parameter in (37). Note that $\xi \cdot \text{pen}(\mathcal{X}) = \lambda \|\mathcal{B}\|_0 + \xi r n_1 n_3 \log_2(\vartheta)$. Then the minimizer $\tilde{\mathcal{X}}^\lambda$ in (2) is the same as the minimizer \mathcal{X}^ξ in (37). Therefore, by Lemma A.1, for any $\xi \geq 2(1 + \frac{2\kappa}{3})\log(2)$, we get that

$$\begin{aligned} & \frac{\mathbb{E}_{\Omega, \mathcal{Y}_\Omega} [-2 \log H(p_{\tilde{\mathcal{X}}^\lambda}, p_{\mathcal{X}^*})]}{n_1 n_2 n_3} \\ & \leq 3 \min_{\mathcal{X} \in \Gamma} \left\{ \frac{D(p_{\mathcal{X}^*} \| p_{\mathcal{X}})}{n_1 n_2 n_3} + \left(\xi + \frac{4\kappa \log(2)}{3} \right) \frac{\text{pen}(\mathcal{X})}{m} \right\} + \frac{8\kappa \log(m)}{m} \\ & \leq 3 \min_{\mathcal{X} \in \Gamma} \left\{ \frac{D(p_{\mathcal{X}^*} \| p_{\mathcal{X}})}{n_1 n_2 n_3} + \left(\xi + \frac{4\kappa \log(2)}{3} \right) \left(\log_2(\vartheta) + \log_2(\tilde{\vartheta}) \right) \frac{r n_1 n_3 + \|\mathcal{B}\|_0}{m} \right\} + \frac{8\kappa \log(m)}{m} \\ & = 3 \min_{\mathcal{X} \in \Gamma} \left\{ \frac{D(p_{\mathcal{X}^*} \| p_{\mathcal{X}})}{n_1 n_2 n_3} + \left(\lambda + \frac{4\kappa \log(2)}{3} \left(\log_2(\vartheta) + \log_2(\tilde{\vartheta}) \right) \right) \frac{r n_1 n_3 + \|\mathcal{B}\|_0}{m} \right\} + \frac{8\kappa \log(m)}{m}, \end{aligned} \quad (40)$$

where the second inequality holds by the definition of $\text{pen}(\mathcal{X})$ and the nonnegativity of $\log_2(\vartheta)$ and $\log_2(\tilde{\vartheta})$. Note that

$$\log_2(\vartheta) + \log_2(\tilde{\vartheta}) \leq 2\beta \log_2(n_1 \vee n_2) + 2\log_2(r n_2) \leq \frac{2(\beta + 2) \log(n_1 \vee n_2)}{\log(2)}, \quad (41)$$

where the last inequality follows from $r n_2 \leq (n_1 \vee n_2)^2$. Hence, for any

$$\lambda \geq 4(\beta + 2) \left(1 + \frac{2\kappa}{3} \right) \log(n_1 \vee n_2),$$

which is equivalent to $\xi \geq 2(1 + \frac{2\kappa}{3})\log(2)$, we have

$$\begin{aligned} & \frac{\mathbb{E}_{\Omega, \mathcal{Y}_\Omega} [-2 \log H(p_{\tilde{\mathcal{X}}^\lambda}, p_{\mathcal{X}^*})]}{n_1 n_2 n_3} \\ & \leq 3 \min_{\mathcal{X} \in \Gamma} \left\{ \frac{D(p_{\mathcal{X}^*} \| p_{\mathcal{X}})}{n_1 n_2 n_3} + \left(\lambda + \frac{8\kappa(\beta + 2) \log(n_1 \vee n_2)}{3} \right) \frac{r n_1 n_3 + \|\mathcal{B}\|_0}{m} \right\} + \frac{8\kappa \log(m)}{m}, \end{aligned}$$

where the inequality follows from (40) and (41). This completes the proof.

APPENDIX B PROOF OF PROPOSITION 4.1

By Theorem 4.1, we only need to give the lower bound of $\mathbb{E}_{\Omega, \mathcal{Y}_\Omega} [-2 \log H(p_{\tilde{\mathcal{X}}^\lambda}, p_{\mathcal{X}^*})]$ and upper bound of $\min_{\mathcal{X} \in \Gamma} \left\{ \frac{D(p_{\mathcal{X}^*} \| p_{\mathcal{X}})}{n_1 n_2 n_3} \right\}$, respectively. It follows from [63, Exercise 15.13] that the KL divergence of two Gaussian distributions is $D(p_{\mathcal{X}_{ijk}^*} \| p_{\mathcal{X}_{ijk}}) = (\mathcal{X}_{i,j,k}^* - \mathcal{X}_{i,j,k})^2 / (2\sigma^2)$, which yields

$$D(p_{\mathcal{X}^*} \| p_{\mathcal{X}}) = \frac{\|\mathcal{X} - \mathcal{X}^*\|_F^2}{2\sigma^2}. \quad (42)$$

Note that $D(p_{\mathcal{X}_{ijk}^*} \| p_{\mathcal{X}_{ijk}}) \leq c^2 / (2\sigma^2)$ for any $\mathcal{X} \in \Gamma$ and i, j, k . We can choose $\kappa = c^2 / (2\sigma^2)$ based on the assumption in Theorem 4.1. Moreover, by [64, Appendix C], we get that

$$-2 \log(H(p_{\mathcal{X}_{ijk}^*}, p_{\tilde{\mathcal{X}}_{ijk}^\lambda})) = (\tilde{\mathcal{X}}_{ijk}^\lambda - \mathcal{X}_{ijk}^*)^2 / (4\sigma^2),$$

which yields that $-2\log(H(p_{\mathcal{X}^*}, p_{\tilde{\mathcal{X}}^\lambda})) = \frac{\|\tilde{\mathcal{X}}^\lambda - \mathcal{X}^*\|_F^2}{4\sigma^2}$. Therefore, by Theorem 4.1, we get that

$$\begin{aligned} & \frac{\mathbb{E}_{\Omega, \mathcal{Y}_\Omega} \left[\|\tilde{\mathcal{X}}^\lambda - \mathcal{X}^*\|_F^2 \right]}{n_1 n_2 n_3} \\ & \leq 3 \min_{\mathcal{X} \in \Gamma} \left\{ \frac{2\|\mathcal{X} - \mathcal{X}^*\|_F^2}{n_1 n_2 n_3} + 4\sigma^2 \left(\lambda + \frac{4c^2(\beta + 2)\log(n_1 \vee n_2)}{3\sigma^2} \right) \frac{rn_1 n_3 + \|\mathcal{B}\|_0}{m} \right\} \\ & \quad + \frac{16c^2 \log(m)}{m}. \end{aligned} \quad (43)$$

Next we need to establish an upper bound of $\min_{\mathcal{X} \in \Gamma} \|\mathcal{X} - \mathcal{X}^*\|_F^2$. Note that

$$\begin{aligned} \vartheta &= 2^{\lceil \log_2(n_1 \vee n_2)^\beta \rceil} \geq 2^{\beta \log_2(n_1 \vee n_2)} \\ &\geq 2^{\log_2(n_1 \vee n_2)} \cdot 2^{\log_2(n_1 \vee n_2) \frac{\log(3rn_3^{1.5}b/c)}{\log(n_1 \vee n_2)}} \\ &= \frac{3(n_1 \vee n_2)rn_3^{1.5}b}{c}, \end{aligned} \quad (44)$$

where the second inequality holds by (5). Since $n_1, n_2 \geq 2$, we have $\vartheta \geq \frac{6rn_3^{1.5}b}{c}$, which implies that $\|\tilde{\mathcal{X}}^*\|_\infty \leq \frac{3rn_3b}{\vartheta} + \|\mathcal{X}^*\|_\infty \leq c$ by Lemma A.2, where $\tilde{\mathcal{X}}^*$ is defined in Lemma A.2. Therefore, $\tilde{\mathcal{X}}^* = \tilde{\mathcal{A}}^* \diamond \tilde{\mathcal{B}}^* \in \Gamma$. By Lemma A.2, we have that

$$\min_{\mathcal{X} \in \Gamma} \left\{ \frac{2\|\mathcal{X} - \mathcal{X}^*\|_F^2}{n_1 n_2 n_3} \right\} \leq \frac{2\|\tilde{\mathcal{X}}^* - \mathcal{X}^*\|_F^2}{n_1 n_2 n_3} \leq \frac{18(rn_3b)^2}{\vartheta^2} \leq \frac{2c^2}{m}, \quad (45)$$

where the last inequality follows from the fact $m \leq (n_1 \vee n_2)^2 n_3$ and (44). Moreover, it follows from the construction of $\tilde{\mathcal{B}}^*$ in Lemma A.2 that $\|\tilde{\mathcal{B}}^*\|_0 = \|\mathcal{B}^*\|_0$. As a consequence, combining (6), (43) with (45), we obtain that

$$\begin{aligned} & \frac{\mathbb{E}_{\Omega, \mathcal{Y}_\Omega} \left[\|\tilde{\mathcal{X}}^\lambda - \mathcal{X}^*\|_F^2 \right]}{n_1 n_2 n_3} \\ & \leq \frac{6c^2}{m} + 16(3\sigma^2 + 2c^2)(\beta + 2) \log((n_1 \vee n_2)\sqrt{n_3}) \left(\frac{rn_1 n_3 + \|\mathcal{B}^*\|_0}{m} \right) + \frac{16c^2 \log(m)}{m} \\ & \leq \frac{22c^2 \log(m)}{m} + 16(3\sigma^2 + 2c^2)(\beta + 2) \left(\frac{rn_1 n_3 + \|\mathcal{B}^*\|_0}{m} \right) \log(n_1 \vee n_2). \end{aligned}$$

This completes the proof.

APPENDIX C

PROOF OF PROPOSITION 4.2

A random variable is said to have a Laplace distribution, denoted by $\text{Laplace}(\mu, b)$ with parameters $b > 0, \mu$, if its probability density function is $f(x|\mu, b) = \frac{1}{2b} \exp(-\frac{|x-\mu|}{b})$. Before deriving the upper bound of observations with additive Laplace noise, we establish the KL divergence and logarithmic Hellinger affinity between two distributions.

Lemma C.1: Let $p(x) \sim \text{Laplace}(\mu_1, b_1)$ and $q(x) \sim \text{Laplace}(\mu_2, b_2)$. Then

$$D(p(x)||q(x)) = \log\left(\frac{b_2}{b_1}\right) + \frac{|\mu_2 - \mu_1|}{b_2} + \frac{b_1}{b_2} \exp\left(-\frac{|\mu_2 - \mu_1|}{b_1}\right).$$

Moreover, if $b_1 = b_2$, then

$$-2 \log(H(p(x), q(x))) = \frac{|\mu_2 - \mu_1|}{b_1} - 2 \log \left(1 + \frac{|\mu_2 - \mu_1|}{2b_1} \right).$$

Proof: By the definition of the KL divergence of $p(x)$ from $q(x)$, we deduce

$$\begin{aligned} D(p(x)||q(x)) &= \mathbb{E}_p [\log(p(x)) - \log(q(x))] \\ &= \log \left(\frac{b_2}{b_1} \right) - \frac{1}{b_1} \mathbb{E}_p[|x - \mu_1|] + \frac{1}{b_2} \mathbb{E}_p[|x - \mu_2|]. \end{aligned}$$

Without loss of generality, we assume that $\mu_1 < \mu_2$. By direct calculations, one can get that $\mathbb{E}_p[|x - \mu_1|] = b_1$ and $\mathbb{E}_p[|x - \mu_2|] = \mu_2 - \mu_1 + b_1 \exp(-\frac{\mu_2 - \mu_1}{b_1})$. Then, we get that

$$D(p(x)||q(x)) = \log \left(\frac{b_2}{b_1} \right) - 1 + \frac{\mu_2 - \mu_1}{b_2} + \frac{b_1 \exp(-\frac{\mu_2 - \mu_1}{b_1})}{b_2}.$$

Therefore, by the symmetry, for any μ_1, μ_2 , we have

$$D(p(x)||q(x)) = \log \left(\frac{b_2}{b_1} \right) - 1 + \frac{|\mu_2 - \mu_1|}{b_2} + \frac{b_1 \exp \left(-\frac{|\mu_2 - \mu_1|}{b_1} \right)}{b_2}.$$

Moreover, if $b_1 = b_2$, the Hellinger affinity is

$$H(p(x), q(x)) = \frac{1}{2b_1} \int_{-\infty}^{+\infty} \exp \left(-\frac{|x - \mu_1|}{2b_1} - \frac{|x - \mu_2|}{2b_1} \right) dx.$$

With simple manipulations, we obtain

$$-2 \log(H(p(x), q(x))) = \frac{|\mu_2 - \mu_1|}{b_1} - 2 \log \left(1 + \frac{|\mu_2 - \mu_1|}{2b_1} \right).$$

The proof is completed. ■

Now we return to prove Proposition 4.2. By Lemma C.1, we have that

$$D(p_{\mathcal{X}_{ijk}^*} || p_{\mathcal{X}_{ijk}}) = \frac{|\mathcal{X}_{ijk}^* - \mathcal{X}_{ijk}|}{\tau} - \left(1 - \exp \left(-\frac{|\mathcal{X}_{ijk}^* - \mathcal{X}_{ijk}|}{\tau} \right) \right) \leq \frac{1}{2\tau^2} (\mathcal{X}_{ijk}^* - \mathcal{X}_{ijk})^2, \quad (46)$$

where the inequality follows from the fact that $e^{-x} \leq 1 - x + \frac{x^2}{2}$ for $x > 0$. Hence, we choose $\kappa = \frac{c^2}{2\tau^2}$. Notice that

$$\begin{aligned} -2 \log(H(p_{\mathcal{X}_{ijk}^*}, p_{\mathcal{X}_{ijk}})) &= \frac{|\mathcal{X}_{ijk}^* - \mathcal{X}_{ijk}|}{\tau} - 2 \log \left(1 + \frac{|\mathcal{X}_{ijk}^* - \mathcal{X}_{ijk}|}{2\tau} \right) \\ &\geq \frac{2(\mathcal{X}_{ijk}^* - \mathcal{X}_{ijk})^2}{(2\tau + c)^2}, \end{aligned}$$

where the last inequality follows from the Taylor's expansion, see also the proof of Corollary 5 in [20]. Therefore, we have $D(p_{\mathcal{X}^*} || p_{\mathcal{X}}) \leq \frac{1}{2\tau^2} \|\mathcal{X}^* - \mathcal{X}\|_F^2$ and

$$-2 \log(A(p_{\mathcal{X}^*}, p_{\mathcal{X}})) \geq \frac{2}{(2\tau + c)^2} \|\mathcal{X}^* - \mathcal{X}\|_F^2.$$

It follows from Theorem 4.1 that

$$\begin{aligned} & \frac{\mathbb{E}_{\Omega, \mathcal{Y}_\Omega} \left[\|\tilde{\mathcal{X}}^\lambda - \mathcal{X}^*\|_F^2 \right]}{n_1 n_2 n_3} \\ & \leq \frac{3(2\tau + c)^2}{2} \cdot \min_{\mathcal{X} \in \Gamma} \left\{ \frac{\|\mathcal{X}^* - \mathcal{X}\|_F^2}{2\tau^2 n_1 n_2 n_3} + \left(\lambda + \frac{4c^2(\beta + 2) \log(n_1 \vee n_2)}{3\tau^2} \right) \frac{rn_1 n_3 + \|\mathcal{B}\|_0}{m} \right\} \\ & \quad + \frac{2c^2(2\tau + c)^2 \log(m)}{m\tau^2}. \end{aligned} \quad (47)$$

For the discretized surrogate $\tilde{\mathcal{X}}^*$ of \mathcal{X}^* , by Lemma A.2, we get

$$\min_{\mathcal{X} \in \Gamma} \left\{ \frac{\|\mathcal{X}^* - \mathcal{X}\|_F^2}{2\tau^2 n_1 n_2 n_3} \right\} \leq \frac{\|\tilde{\mathcal{X}}^* - \mathcal{X}^*\|_F^2}{2\tau^2 n_1 n_2 n_3} \leq \frac{(3rn_3 b)^2}{2\tau^2 \vartheta^2} \leq \frac{c^2}{2\tau^2 (n_1 \vee n_2)^2 n_3} \leq \frac{c^2}{2\tau^2 m},$$

where the third inequality follows from (44) and the last inequality follows from the fact that $m \leq (n_1 \vee n_2)^2 n_3$. Note that $\|\tilde{\mathcal{B}}^*\|_0 = \|\mathcal{B}^*\|_0$ by the construction of $\tilde{\mathcal{X}}^*$ in Lemma A.2. Combining (47) with (6), we obtain that

$$\begin{aligned} & \frac{\mathbb{E}_{\Omega, \mathcal{Y}_\Omega} \left[\|\tilde{\mathcal{X}}^\lambda - \mathcal{X}^*\|_F^2 \right]}{n_1 n_2 n_3} \\ & \leq \frac{3c^2(2\tau + c)^2}{4m\tau^2} + 2 \left(3 + \frac{c^2}{\tau^2} \right) (2\tau + c)^2 (\beta + 2) \log(n_1 \vee n_2) \left(\frac{rn_1 n_3 + \|\mathcal{B}^*\|_0}{m} \right) \\ & \quad + \frac{2c^2(2\tau + c)^2 \log(m)}{m\tau^2} \\ & \leq \frac{3c^2(2\tau + c)^2 \log(m)}{m\tau^2} + 2 \left(3 + \frac{c^2}{\tau^2} \right) (2\tau + c)^2 (\beta + 2) \left(\frac{rn_1 n_3 + \|\mathcal{B}^*\|_0}{m} \right) \log(n_1 \vee n_2). \end{aligned}$$

This completes the proof.

APPENDIX D PROOF OF PROPOSITION 4.3

For the KL divergence of Poisson observations, it follows from [53, Lemma 8] that

$$D(p_{\mathcal{X}_{ijk}^*} \| p_{\mathcal{X}_{ijk}}) \leq \frac{1}{\mathcal{X}_{ijk}} (\mathcal{X}_{ijk}^* - \mathcal{X}_{ijk})^2 \leq \frac{1}{\zeta} (\mathcal{X}_{ijk}^* - \mathcal{X}_{ijk})^2. \quad (48)$$

Then we can choose $\kappa = \frac{c^2}{\zeta}$. Note that

$$(\mathcal{X}_{ijk}^* - \mathcal{X}_{ijk})^2 = \left(\left(\sqrt{\mathcal{X}_{ijk}^*} - \sqrt{\mathcal{X}_{ijk}} \right) \left(\sqrt{\mathcal{X}_{ijk}^*} + \sqrt{\mathcal{X}_{ijk}} \right) \right)^2 \leq 4c \left(\sqrt{\mathcal{X}_{ijk}^*} - \sqrt{\mathcal{X}_{ijk}} \right)^2.$$

Therefore, by [49, Appendix IV], we have

$$-2 \log(H(p_{\mathcal{X}_{ijk}^*}, p_{\mathcal{X}_{ijk}})) = \left(\sqrt{\mathcal{X}_{ijk}^*} - \sqrt{\mathcal{X}_{ijk}} \right)^2 \geq \frac{1}{4c} (\mathcal{X}_{ijk}^* - \mathcal{X}_{ijk})^2. \quad (49)$$

Therefore, we get $D(p_{\mathcal{X}^*} \| p_{\mathcal{X}}) \leq \frac{\|\mathcal{X}^* - \mathcal{X}\|_F^2}{\zeta}$ and $-2 \log(A(p_{\mathcal{X}^*}, p_{\mathcal{X}})) \geq \frac{1}{4c} \|\mathcal{X}^* - \mathcal{X}\|_F^2$. For the discreteized surrogate $\tilde{\mathcal{X}}^* = \tilde{\mathcal{A}}^* \diamond \tilde{\mathcal{B}}^*$ of \mathcal{X}^* , by Lemma A.2, we have

$$\min_{\mathcal{X} \in \Gamma} \left\{ \frac{\|\mathcal{X} - \mathcal{X}^*\|_F^2}{\zeta n_1 n_2 n_3} \right\} \leq \frac{\|\tilde{\mathcal{X}}^* - \mathcal{X}^*\|_F^2}{\zeta n_1 n_2 n_3} \leq \frac{9(rn_3 b)^2}{\zeta \vartheta^2} \leq \frac{c^2}{\zeta (n_1 \vee n_2)^2 n_3} \leq \frac{c^2}{\zeta m}, \quad (50)$$

where the third inequality follows from (44). Notice that $\|\tilde{\mathcal{B}}^*\|_0 = \|\mathcal{B}^*\|_0$. Therefore, combining (49), (50), and Theorem 4.1, we conclude

$$\begin{aligned} & \frac{\mathbb{E}_{\Omega, \mathcal{Y}_\Omega} \|\tilde{\mathcal{X}}^\lambda - \tilde{\mathcal{X}}^*\|_F^2}{n_1 n_2 n_3} \\ & \leq \frac{12c^3}{\zeta m} + 12c \left(\lambda + \frac{8\kappa(\beta + 2) \log(n_1 \vee n_2)}{3} \right) \frac{r n_1 n_3 + \|\mathcal{B}^*\|_0}{m} + \frac{32c^3 \log(m)}{\zeta m} \\ & = \frac{4c^3(3 + 8 \log(m))}{\zeta m} + 48c \left(1 + \frac{4c^2}{3\zeta} \right) \frac{(\beta + 2)(r n_1 n_3 + \|\mathcal{B}^*\|_0) \log(n_1 \vee n_2)}{m}, \end{aligned}$$

where the equality follows from (6). The proof is completed.

APPENDIX E PROOF OF THEOREM 5.1

Let

$$\mathfrak{X} := \{\mathcal{X} = \mathcal{A} \diamond \mathcal{B} : \mathcal{A} \in \mathfrak{C}, \mathcal{B} \in \mathfrak{B}\}, \quad (51)$$

where $\mathfrak{C} \subseteq \mathbb{R}^{n_1 \times r \times n_3}$ is defined as

$$\mathfrak{C} := \{\mathcal{A} \in \mathbb{R}^{n_1 \times r \times n_3} : \mathcal{A}_{ijk} \in \{0, 1, a_0\}\} \quad \text{with} \quad a_0 = \min \left\{ 1, \frac{\beta_a \nu}{b \sqrt{\Delta}} \sqrt{\frac{r n_1 n_3}{m}} \right\}, \quad (52)$$

and \mathfrak{B} is defined as

$$\mathfrak{B} := \{\mathcal{B} \in \mathbb{R}^{r \times n_2 \times n_3} : \mathcal{B}_{ijk} \in \{0, b, b_0\}, \|\mathcal{B}\|_0 \leq s\} \quad \text{with} \quad b_0 = \min \left\{ b, \frac{\beta_b \nu}{\sqrt{\Delta}} \sqrt{\frac{s}{m}} \right\}. \quad (53)$$

Here $\beta_a, \beta_b > 0$ are two constants which will be defined later. From the construction, we get that $\mathfrak{X} \subseteq \mathfrak{U}(r, b, s)$.

Now we define a subset $\mathfrak{X}_{\mathcal{A}}$ such that $\mathfrak{X}_{\mathcal{A}} \subseteq \mathfrak{X}$. Denote

$$\mathfrak{X}_{\mathcal{A}} := \left\{ \mathcal{X} := \mathcal{A} \diamond \tilde{\mathcal{B}} : \mathcal{A} \in \tilde{\mathfrak{C}}, \tilde{\mathcal{B}} = b(\mathcal{I}_r \cdots \mathcal{I}_r \mathbf{0}_B) \in \mathfrak{B} \right\}, \quad (54)$$

where $\tilde{\mathcal{B}}$ is a block tensor with $\lfloor \frac{s \wedge (n_2 n_3)}{r n_3} \rfloor$ blocks \mathcal{I}_r , $\mathcal{I}_r \in \mathbb{R}^{r \times r \times n_3}$ is the identity tensor, $\mathbf{0}_B \in \mathbb{R}^{r \times (n_2 - \lfloor \frac{s \wedge (n_2 n_3)}{r n_3} \rfloor r) \times n_3}$ is the zero tensor with all entries being zero, and

$$\tilde{\mathfrak{C}} := \{\mathcal{A} \in \mathbb{R}^{n_1 \times r \times n_3} : \mathcal{A}_{ijk} \in \{0, a_0\}, 1 \leq i \leq n_1, 1 \leq j \leq r, 1 \leq k \leq n_3\}. \quad (55)$$

By the definition of identity tensor, we get $\|\tilde{\mathcal{B}}\|_0 = r \lfloor \frac{s \wedge (n_2 n_3)}{r n_3} \rfloor \leq r \frac{s \wedge (n_2 n_3)}{r n_3} \leq s$. It follows from the construction of $\tilde{\mathcal{B}} = b(\mathcal{I}_r \cdots \mathcal{I}_r \mathbf{0}_B)$ that $\tilde{\mathcal{B}} \in \mathfrak{B}$. Therefore, $\mathfrak{X}_{\mathcal{A}} \subseteq \mathfrak{X}$. By the definition of tensor-tensor product, we have that

$$\mathcal{A} \diamond \mathcal{I}_r = \text{Fold} \left(\begin{pmatrix} \mathbf{A}^{(1)} & \mathbf{A}^{(n_3)} & \cdots & \mathbf{A}^{(2)} \\ \mathbf{A}^{(2)} & \mathbf{A}^{(1)} & \cdots & \mathbf{A}^{(3)} \\ \vdots & \vdots & \ddots & \vdots \\ \mathbf{A}^{(n_3)} & \mathbf{A}^{(n_3-1)} & \cdots & \mathbf{A}^{(1)} \end{pmatrix} \cdot \begin{pmatrix} \mathbf{I}_r \\ \mathbf{0} \\ \vdots \\ \mathbf{0} \end{pmatrix} \right) = \text{Fold} \begin{pmatrix} \mathbf{A}^{(1)} \\ \mathbf{A}^{(2)} \\ \vdots \\ \mathbf{A}^{(n_3)} \end{pmatrix} = \mathcal{A},$$

where \mathbf{I}_r is the $r \times r$ identity matrix. Hence, for any $\mathcal{X} \in \mathfrak{X}_{\mathcal{A}}$, we have that

$$\mathcal{X} = b\mathcal{A} \diamond (\mathcal{I}_r \cdots \mathcal{I}_r \mathbf{0}_B) = b(\mathcal{A} \cdots \mathcal{A} \mathbf{0}_{\mathcal{X}}),$$

where $\mathbf{0}_{\mathcal{X}} \in \mathbb{R}^{n_1 \times (n_2 - \lfloor \frac{s \wedge (n_2 n_3)}{r n_3} \rfloor r) \times n_3}$ is a zero tensor. Notice that each entry of \mathcal{A} is 0 or a_0 . Therefore, by the Varshamov-Gilbert bound [55, Lemma 2.9], we have that there exists a subset $\mathfrak{X}_{\mathcal{A}}^0 \subseteq \mathfrak{X}_{\mathcal{A}}$ with $|\mathfrak{X}_{\mathcal{A}}^0| \geq 2^{rn_1 n_3/8} + 1$, such that for any $\mathcal{X}_i, \mathcal{X}_j \in \mathfrak{X}_{\mathcal{A}}^0$,

$$\begin{aligned} \|\mathcal{X}_i - \mathcal{X}_j\|_F^2 &\geq \frac{rn_1 n_3}{8} \left\lfloor \frac{s \wedge (n_2 n_3)}{r n_3} \right\rfloor a_0^2 b^2 \\ &\geq \frac{n_1 n_2 n_3}{16} \min \left\{ b^2 \Delta, \beta_a^2 \nu^2 \frac{rn_1 n_3}{m} \right\}, \end{aligned} \quad (56)$$

where the last inequality of (56) holds by $\lfloor x \rfloor \geq \frac{x}{2}$ for any $x \geq 1$. For any $\mathcal{X} \in \mathfrak{X}_{\mathcal{A}}^0$, we have that

$$\begin{aligned} D(p_{\mathcal{X}_{\Omega}}(\mathcal{Y}_{\Omega}) || p_{\mathbf{0}_{\Omega}}(\mathcal{Y}_{\Omega})) &= \frac{m}{n_1 n_2 n_3} \sum_{i,j,k} D(p_{\mathcal{X}_{ijk}}(\mathcal{Y}_{ijk}) || p_{\mathbf{0}_{ijk}}(\mathcal{Y}_{ijk})) \\ &\leq \frac{m}{n_1 n_2 n_3} \sum_{i,j,k} \frac{1}{2\nu^2} |\mathcal{X}_{ijk}|^2 \\ &\leq \frac{m}{n_1 n_2 n_3} \frac{1}{2\nu^2} (rn_1 n_3) \left\lfloor \frac{s \wedge (n_2 n_3)}{r n_3} \right\rfloor a_0^2 b^2 \\ &\leq \frac{m}{2\nu^2} \min \left\{ \Delta b^2, \beta_a^2 \nu^2 \frac{rn_1 n_3}{m} \right\}, \end{aligned} \quad (57)$$

where the first inequality follows from (21), the second inequality follows from $|\mathcal{X}_{ijk}| \leq b \|\mathcal{A}\|_{\infty}$, and the last inequality follows from (52). Therefore, combining (52) with (57), we get that

$$\sum_{\mathcal{X} \in \mathfrak{X}_{\mathcal{A}}^0} D(p_{\mathcal{X}_{\Omega}}(\mathcal{Y}_{\Omega}) || p_{\mathbf{0}_{\Omega}}(\mathcal{Y}_{\Omega})) \leq (|\mathfrak{X}_{\mathcal{A}}^0| - 1) \frac{\beta_a^2 r n_1 n_3}{2} \leq (|\mathfrak{X}_{\mathcal{A}}^0| - 1) \frac{4\beta_a^2 \log(|\mathfrak{X}_{\mathcal{A}}^0| - 1)}{\log(2)},$$

where the last inequality holds by $rn_1 n_3 \leq 8 \log_2(|\mathfrak{X}_{\mathcal{A}}^0| - 1)$. Therefore, by choosing $0 < \beta_a \leq \frac{\sqrt{\alpha_1 \log(2)}}{2}$ with $0 < \alpha_1 < \frac{1}{8}$, we have

$$\frac{1}{|\mathfrak{X}_{\mathcal{A}}^0| - 1} \sum_{\mathcal{X} \in \mathfrak{X}_{\mathcal{A}}^0} D(p_{\mathcal{X}_{\Omega}}(\mathcal{Y}_{\Omega}) || p_{\mathbf{0}_{\Omega}}(\mathcal{Y}_{\Omega})) \leq \alpha_1 \log(|\mathfrak{X}_{\mathcal{A}}^0| - 1).$$

Hence, by [55, Theorem 2.5], we deduce

$$\begin{aligned} &\inf_{\tilde{\mathcal{X}}} \sup_{\mathcal{X}^* \in \mathfrak{X}_{\mathcal{A}}} \mathbb{P} \left(\frac{\|\tilde{\mathcal{X}} - \mathcal{X}^*\|_F^2}{n_1 n_2 n_3} \geq \frac{1}{32} \min \left\{ b^2 \Delta, \beta_a^2 \nu^2 \frac{rn_1 n_3}{m} \right\} \right) \\ &\geq \inf_{\tilde{\mathcal{X}}} \sup_{\mathcal{X}^* \in \mathfrak{X}_{\mathcal{A}}^0} \mathbb{P} \left(\frac{\|\tilde{\mathcal{X}} - \mathcal{X}^*\|_F^2}{n_1 n_2 n_3} \geq \frac{1}{32} \min \left\{ b^2 \Delta, \beta_a^2 \nu^2 \frac{rn_1 n_3}{m} \right\} \right) \geq \theta_1, \end{aligned} \quad (58)$$

where

$$\theta_1 = \frac{\sqrt{|\mathfrak{X}_{\mathcal{A}}^0| - 1}}{1 + \sqrt{|\mathfrak{X}_{\mathcal{A}}^0| - 1}} \left(1 - 2\alpha_1 - \sqrt{\frac{2\alpha_1}{\log(|\mathfrak{X}_{\mathcal{A}}^0| - 1)}} \right) \in (0, 1).$$

Similar to the previous discussion, we construct $\mathfrak{X}_{\mathcal{B}}$ as follows:

$$\mathfrak{X}_{\mathcal{B}} := \left\{ \mathcal{X} = \tilde{\mathcal{A}} \diamond \mathcal{B} : \mathcal{B} \in \tilde{\mathfrak{B}} \right\}, \quad (59)$$

where $\tilde{\mathcal{A}}$ is a block tensor defined as

$$\tilde{\mathcal{A}} := \begin{pmatrix} \mathcal{I}_{r'} & \mathbf{0} \\ \vdots & \vdots \\ \mathcal{I}_{r'} & \mathbf{0} \\ \mathbf{0} & \mathbf{0} \end{pmatrix} \in \mathbb{R}^{n_1 \times r \times n_3}$$

and $\tilde{\mathfrak{B}}$ is a set defined as

$$\tilde{\mathfrak{B}} := \left\{ \mathcal{B} \in \mathbb{R}^{r \times n_2 \times n_3} : \mathcal{B} = \begin{pmatrix} \mathcal{B}_{r'} \\ \mathbf{0} \end{pmatrix}, \mathcal{B}_{r'} \in \mathbb{R}^{r' \times n_2 \times n_3}, (\mathcal{B}_{r'})_{ijk} \in \{0, b_0\}, \|\mathcal{B}_{r'}\|_0 \leq s \right\}. \quad (60)$$

Here $r' = \lceil \frac{s}{n_2 n_3} \rceil$, $\mathcal{I}_{r'} \in \mathbb{R}^{r' \times r' \times n_3}$ is the identity tensor, there are $\lfloor \frac{n_1}{r'} \rfloor$ block tensors $\mathcal{I}_{r'}$ in $\tilde{\mathcal{A}}$, and $\mathbf{0}$ is a zero tensor with all entries being zero whose dimension can be known from the context. Thus $\mathfrak{X}_{\tilde{\mathcal{B}}} \subseteq \mathfrak{X}$. Note that

$$\mathcal{I}_{r'} \diamond \mathcal{B}_{r'} = \text{Fold} \left(\begin{pmatrix} \mathbf{I}_{r'} & \mathbf{0} & \cdots & \mathbf{0} \\ \mathbf{0} & \mathbf{I}_{r'} & \cdots & \mathbf{0} \\ \vdots & \vdots & \ddots & \vdots \\ \mathbf{0} & \mathbf{0} & \cdots & \mathbf{I}_{r'} \end{pmatrix} \cdot \begin{pmatrix} \mathbf{B}_{r'}^{(1)} \\ \mathbf{B}_{r'}^{(2)} \\ \vdots \\ \mathbf{B}_{r'}^{(n_3)} \end{pmatrix} \right) = \text{Fold} \begin{pmatrix} \mathbf{B}_{r'}^{(1)} \\ \mathbf{B}_{r'}^{(2)} \\ \vdots \\ \mathbf{B}_{r'}^{(n_3)} \end{pmatrix} = \mathcal{B}_{r'}.$$

For any $\mathcal{X} \in \mathfrak{X}_{\tilde{\mathcal{B}}}$, we have

$$\mathcal{X} = \begin{pmatrix} \mathcal{I}_{r'} & \mathbf{0} \\ \vdots & \vdots \\ \mathcal{I}_{r'} & \mathbf{0} \\ \mathbf{0} & \mathbf{0} \end{pmatrix} \diamond \begin{pmatrix} \mathcal{B}_{r'} \\ \mathbf{0} \end{pmatrix} = \begin{pmatrix} \mathcal{B}_{r'} \\ \vdots \\ \mathcal{B}_{r'} \\ \mathbf{0} \end{pmatrix},$$

where $(\mathcal{B}_{r'})_{ijk} \in \{0, b_0\}$, $\|\mathcal{B}_{r'}\|_0 \leq s$, and there are $\lfloor \frac{n_1}{r'} \rfloor$ blocks $\mathcal{B}_{r'}$ in \mathcal{X} . By the Varshamov-Gilbert bound [55, Lemma 2.9], there is a subset $\mathfrak{X}_{\tilde{\mathcal{B}}}^0 \subseteq \mathfrak{X}_{\tilde{\mathcal{B}}}$ such that for any $\mathcal{X}_i, \mathcal{X}_j \in \mathfrak{X}_{\tilde{\mathcal{B}}}^0$,

$$|\mathfrak{X}_{\tilde{\mathcal{B}}}^0| \geq 2^{r' n_2 n_3 / 8} + 1 \geq 2^{s/8} + 1 \quad (61)$$

and

$$\begin{aligned} \|\mathcal{X}_i - \mathcal{X}_j\|_F^2 &\geq \frac{r' n_2 n_3}{8} \left\lfloor \frac{n_1}{r'} \right\rfloor b_0^2 \geq \frac{s}{8} \left\lfloor \frac{n_1}{r'} \right\rfloor b_0^2 \\ &\geq \frac{s n_1}{16 r'} b_0^2 = \frac{n_1 n_2 n_3}{16} \frac{s}{n_2 n_3 \lceil \frac{s}{n_2 n_3} \rceil} b_0^2 \\ &\geq \frac{n_1 n_2 n_3}{16} \min \left\{ \frac{1}{2}, \frac{s}{n_2 n_3} \right\} b_0^2 \geq \frac{n_1 n_2 n_3}{32} \Delta \min \left\{ b^2, \frac{\beta_b^2 \nu^2 s}{\Delta m} \right\} \\ &= \frac{n_1 n_2 n_3}{32} \min \left\{ \Delta b^2, \frac{\beta_b^2 \nu^2 s}{m} \right\}, \end{aligned}$$

where the third inequality follows from $\lfloor x \rfloor \geq \frac{x}{2}$ for any $x \geq 1$ and the fourth inequality follows from the fact that $\frac{x}{\lceil x \rceil} \geq \min\{\frac{1}{2}, x\}$ for any $x > 0$.

For any $\mathcal{X} \in \mathfrak{X}_B^0$, the KL divergence of observations with parameters \mathcal{X}_Ω from $\mathbf{0}_\Omega$ is given by

$$\begin{aligned} D(p_{\mathcal{X}_\Omega}(\mathcal{Y}_\Omega) || p_{\mathbf{0}_\Omega}(\mathcal{Y}_\Omega)) &= \frac{m}{n_1 n_2 n_3} \sum_{i,j,k} D(p_{\mathcal{X}_{ijk}}(\mathcal{Y}_{ijk}) || p_{\mathbf{0}_{ijk}}(\mathcal{Y}_{ijk})) \leq \frac{m}{2\nu^2 n_1 n_2 n_3} \sum_{i,j,k} |\mathcal{X}_{ijk}|^2 \\ &\leq \frac{m}{2\nu^2 n_1 n_2 n_3} n_1 (s \wedge (n_2 n_3)) b_0^2 = \frac{m}{2\nu^2} \min \left\{ \Delta b^2, \frac{\beta_b^2 \nu^2 s}{m} \right\} \\ &\leq \frac{\beta_b^2 s}{2} \leq 4\beta_b^2 \frac{\log(|\mathfrak{X}_B^0| - 1)}{\log(2)}, \end{aligned}$$

where the second inequality follows from the fact that the nonzero entries of \mathcal{X} is not larger than $s \lfloor \frac{n_1}{r'} \rfloor = n_1 (s \wedge (n_2 n_3))$, and the last inequality holds by $s \leq 8 \log_2(|\mathfrak{X}_B^0| - 1)$. By choosing $0 < \beta_b \leq \frac{\sqrt{\alpha_2 \log(2)}}{2}$ with $0 < \alpha_2 < \frac{1}{8}$, we obtain that

$$\frac{1}{|\mathfrak{X}_B^0| - 1} \sum_{\mathcal{X} \in \mathfrak{X}_B^0} D(p_{\mathcal{X}_\Omega}(\mathcal{Y}_\Omega) || p_{\mathbf{0}_\Omega}(\mathcal{Y}_\Omega)) \leq \alpha_2 \log(|\mathfrak{X}_B^0| - 1).$$

Therefore, by [55, Theorem 2.5], we have that

$$\begin{aligned} &\inf_{\tilde{\mathcal{X}}} \sup_{\mathcal{X}^* \in \mathfrak{X}_B} \mathbb{P} \left(\frac{\|\tilde{\mathcal{X}} - \mathcal{X}^*\|_F^2}{n_1 n_2 n_3} \geq \frac{1}{32} \min \left\{ \Delta b^2, \frac{\beta_b^2 \nu^2 s}{m} \right\} \right) \\ &\geq \inf_{\tilde{\mathcal{X}}} \sup_{\mathcal{X}^* \in \mathfrak{X}_B^0} \mathbb{P} \left(\frac{\|\tilde{\mathcal{X}} - \mathcal{X}^*\|}{n_1 n_2 n_3} \geq \frac{1}{32} \min \left\{ \Delta b^2, \frac{\beta_b^2 \nu^2 s}{m} \right\} \right) \geq \theta_2, \end{aligned} \tag{62}$$

where

$$\theta_2 = \frac{\sqrt{|\mathfrak{X}_B^0| - 1}}{1 + \sqrt{|\mathfrak{X}_B^0| - 1}} \left(1 - 2\alpha_2 - \sqrt{\frac{2\alpha_2}{\log(|\mathfrak{X}_B^0| - 1)}} \right) \in (0, 1).$$

Let $\beta_c = \min\{\beta_a, \beta_b\}$ and $\theta_c = \min\{\theta_1, \theta_2\}$. Combining (58) and (62), we deduce

$$\inf_{\tilde{\mathcal{X}}} \sup_{\mathcal{X}^* \in \mathfrak{U}(r,b,k)} \mathbb{P} \left(\frac{\|\tilde{\mathcal{X}} - \mathcal{X}^*\|_F^2}{n_1 n_2 n_3} \geq \frac{1}{64} \min \left\{ \Delta b^2, \beta_c^2 \nu^2 \left(\frac{s + r n_1 n_3}{m} \right) \right\} \right) \geq \theta_c.$$

By Markov's inequality, we conclude

$$\inf_{\tilde{\mathcal{X}}} \sup_{\mathcal{X}^* \in \mathfrak{U}(r,b,k)} \frac{\mathbb{E}_{\Omega, \mathcal{Y}_\Omega} \|\tilde{\mathcal{X}} - \mathcal{X}^*\|_F^2}{n_1 n_2 n_3} \geq \frac{\theta_c}{64} \min \left\{ \Delta b^2, \beta_c^2 \nu^2 \left(\frac{s + r n_1 n_3}{m} \right) \right\}.$$

This completes the proof.

APPENDIX F PROOF OF PROPOSITION 5.1

By (42), we choose $\nu = \sigma$. It follows from Theorem 5.1 that we can get the desired result.

APPENDIX G PROOF OF PROPOSITION 5.2

By (46), we can choose $\nu = \tau$. Then the conclusion can be obtained easily by Theorem 5.1.

APPENDIX H
PROOF OF PROPOSITION 5.3

Let

$$\mathfrak{X}_1 := \{\mathcal{X} = \mathcal{A} \diamond \mathcal{B} : \mathcal{A} \in \mathfrak{C}_1, \mathcal{B} \in \mathfrak{B}_1\}, \quad (63)$$

where $\mathfrak{C}_1 \subseteq \mathbb{R}^{n_1 \times r \times n_3}$ is defined as

$$\mathfrak{C}_1 := \{\mathcal{A} \in \mathbb{R}^{n_1 \times r \times n_3} : \mathcal{A}_{ijk} \in \{0, 1, \varsigma, a_0\}\} \quad \text{with } a_0 = \min \left\{ 1 - \varsigma, \frac{\beta_a \sqrt{\zeta}}{b} \sqrt{\frac{rn_1 n_3}{m}} \right\}, \quad (64)$$

and \mathfrak{B} is defined as

$$\mathfrak{B}_1 := \{\mathcal{B} \in \mathbb{R}^{r \times n_2 \times n_3} : \mathcal{B}_{ijk} \in \{0, \zeta, b, b_0\}, \|\mathcal{B}\|_0 \leq s\} \quad \text{with } b_0 = \min \left\{ b, \beta_b \sqrt{\frac{\zeta}{\Delta_1}} \sqrt{\frac{s - n_2 n_3}{m}} \right\}. \quad (65)$$

Let

$$\tilde{\mathfrak{X}}_{\mathcal{A}} := \left\{ \mathcal{X} := (\mathcal{A} + \mathcal{A}_{\varsigma}) \diamond \mathcal{B} : \mathcal{A} \in \tilde{\mathfrak{C}}_1, \mathcal{B} = b(\mathcal{I}_r \cdots \mathcal{I}_r \mathcal{B}_{\mathcal{I}}) \in \mathfrak{B}_1 \right\}, \quad (66)$$

where $\mathcal{I}_r \in \mathbb{R}^{r \times r \times n_3}$ is the identity tensor, there are $\lfloor \frac{n_2}{r} \rfloor$ blocks \mathcal{I}_r in \mathcal{B} , $\mathcal{B}_{\mathcal{I}} = \begin{pmatrix} \mathcal{I}_{\mathcal{B}} \\ \mathbf{0} \end{pmatrix}$, $\mathcal{I}_{\mathcal{B}} \in \mathbb{R}^{(n_2 - r \lfloor \frac{n_2}{r} \rfloor) \times (n_2 - r \lfloor \frac{n_2}{r} \rfloor) \times n_3}$ is the identity tensor, $\mathcal{A}_{\varsigma} \in \mathbb{R}^{n_1 \times r \times n_3}$ with $(\mathcal{A}_{\varsigma})_{ijk} = \varsigma$, and

$$\tilde{\mathfrak{C}}_1 := \{\mathcal{A} \in \mathbb{R}^{n_1 \times r \times n_3} : \mathcal{A}_{ijk} \in \{0, a_0\}\} \subseteq \mathfrak{C}_1. \quad (67)$$

From the construction of \mathcal{B} , we know that $\|\mathcal{B}\|_0 = n_2 < s$. For any $\mathcal{X} \in \tilde{\mathfrak{X}}_{\mathcal{A}}$, we obtain that

$$\mathcal{X} = (\mathcal{A} + \mathcal{A}_{\varsigma}) \diamond \mathcal{B} = \zeta \mathbb{I} \diamond (\mathcal{I}_r \cdots \mathcal{I}_r \mathcal{B}_{\mathcal{I}}) + \mathcal{A} \diamond \mathcal{B}, \quad (68)$$

where $\mathbb{I} \in \mathbb{R}^{n_1 \times r \times n_3}$ denotes a tensor with all entries being 1. By the definition of tensor-tensor product, we have that

$$\begin{aligned} \mathbb{I} \diamond (\mathcal{I}_r \cdots \mathcal{I}_r \mathcal{B}_{\mathcal{I}}) &= \text{Fold} \left(\begin{pmatrix} \mathbf{E}_{n_1 r} & \mathbf{E}_{n_1 r} & \cdots & \mathbf{E}_{n_1 r} \\ \mathbf{E}_{n_1 r} & \mathbf{E}_{n_1 r} & \cdots & \mathbf{E}_{n_1 r} \\ \vdots & \vdots & & \vdots \\ \mathbf{E}_{n_1 r} & \mathbf{E}_{n_1 r} & \cdots & \mathbf{E}_{n_1 r} \end{pmatrix} \cdot \begin{pmatrix} \mathbf{I}_r & \mathbf{I}_r & \cdots & \mathbf{I}_r & \mathbf{I}_B \\ \mathbf{0} & \mathbf{0} & \cdots & \mathbf{0} & \mathbf{0} \\ \vdots & \vdots & & \vdots & \vdots \\ \mathbf{0} & \mathbf{0} & \cdots & \mathbf{0} & \mathbf{0} \end{pmatrix} \right) \\ &= \text{Fold} \begin{pmatrix} \mathbf{E}_{n_1 n_2} \\ \mathbf{E}_{n_1 n_2} \\ \vdots \\ \mathbf{E}_{n_1 n_2} \end{pmatrix} = \mathbb{I}_{n_1 n_2}, \end{aligned}$$

where $\mathbf{E}_{n_1 r} \in \mathbb{R}^{n_1 \times r}$ is an $n_1 \times r$ matrix with all entries being 1, \mathbf{I}_r is the $r \times r$ identity matrix, $\mathbf{I}_{B0} = \begin{pmatrix} \mathbf{I}_B \\ \mathbf{0} \end{pmatrix}$ with $\mathbf{I}_B \in \mathbb{R}^{(n_2 - r \lfloor \frac{n_2}{r} \rfloor) \times (n_2 - r \lfloor \frac{n_2}{r} \rfloor)}$ being the identity matrix, and $\mathbb{I}_{n_1 n_2} \in \mathbb{R}^{n_1 \times n_2 \times n_3}$

is a tensor with all entries being 1. Therefore, we have $\tilde{\mathfrak{X}}_{\mathcal{A}} \subseteq \tilde{\mathfrak{U}}(r, b, s, \zeta)$. By applying the Varshamov-Gilbert bound [55, Lemma 2.9] to the last term of (68), there is a subset $\tilde{\mathfrak{X}}_{\mathcal{A}}^0 \subseteq \tilde{\mathfrak{X}}_{\mathcal{A}}$ such that for any $\mathcal{X}_1, \mathcal{X}_2 \in \tilde{\mathfrak{X}}_{\mathcal{A}}^0$,

$$\|\mathcal{X}_1 - \mathcal{X}_2\|_F^2 \geq \frac{rn_1 n_3}{8} \left\lfloor \frac{n_2}{r} \right\rfloor a_0^2 b^2 \geq \frac{n_1 n_2 n_3}{8} \min \left\{ (1 - \varsigma)^2 b^2, \frac{\beta_a^2 \zeta r n_1 n_3}{m} \right\}$$

and $|\tilde{\mathfrak{X}}_{\mathcal{A}}^0| \geq 2^{\frac{rn_1n_3}{8}} + 1$. Let $\mathcal{X}_0 = \zeta \mathbb{I} \diamond (\mathcal{I}_r \cdots \mathcal{I}_r \mathcal{B}_{\mathcal{I}})$. For any $\mathcal{X} \in \tilde{\mathfrak{X}}_{\mathcal{A}}^0$, the KL divergence of $p_{\mathcal{X}_{\Omega}}(\mathcal{Y}_{\Omega})$ from $p_{(\mathcal{X}_0)_{\Omega}}(\mathcal{Y}_{\Omega})$ is

$$\begin{aligned} D(p_{\mathcal{X}_{\Omega}}(\mathcal{Y}_{\Omega}) || p_{(\mathcal{X}_0)_{\Omega}}(\mathcal{Y}_{\Omega})) &= \frac{m}{n_1 n_2 n_3} \sum_{i,j,k} D(p_{\mathcal{X}_{ijk}}(\mathcal{Y}_{ijk}) || p_{(\mathcal{X}_0)_{ijk}}(\mathcal{Y}_{ijk})) \\ &\leq \frac{m}{n_1 n_2 n_3} \sum_{i,j,k} \frac{(\mathcal{X}_{ijk} - \zeta)^2}{\zeta} \\ &\leq \frac{m(a_0 b)^2}{\zeta} \leq \beta_a^2 r n_1 n_3, \end{aligned}$$

where the first inequality follows from (48), the second inequality follows from (68), and the last inequality follows from (64). Note that $rn_1n_3 \leq \frac{8 \log(|\tilde{\mathfrak{X}}_{\mathcal{A}}^0| - 1)}{\log(2)}$. Then, by choosing $0 < \beta_a \leq \frac{\sqrt{\tilde{\alpha}_1 \log(2)}}{2\sqrt{2}}$ and $0 < \tilde{\alpha}_1 < \frac{1}{8}$, we get that

$$\frac{1}{|\tilde{\mathfrak{X}}_{\mathcal{A}}^0| - 1} \sum_{\mathcal{X} \in \tilde{\mathfrak{X}}_{\mathcal{A}}^0} D(p_{\mathcal{X}_{\Omega}}(\mathcal{Y}_{\Omega}) || p_{\mathbf{0}_{\Omega}}(\mathcal{Y}_{\Omega})) \leq \tilde{\alpha}_1 \log(|\tilde{\mathfrak{X}}_{\mathcal{A}}^0| - 1).$$

Therefore, by [55, Theorem 2.5], we have that

$$\begin{aligned} &\inf_{\tilde{X}} \sup_{\mathcal{X}^* \in \tilde{\mathfrak{X}}_{\mathcal{A}}} \mathbb{P} \left(\frac{\|\tilde{\mathcal{X}} - \mathcal{X}^*\|_F^2}{n_1 n_2 n_3} \geq \frac{1}{8} \min \left\{ (1 - \varsigma)^2 b^2, \frac{\beta_a^2 \zeta r n_1 n_3}{m} \right\} \right) \\ &\geq \inf_{\tilde{X}} \sup_{\mathcal{X}^* \in \tilde{\mathfrak{X}}_{\mathcal{A}}^0} \mathbb{P} \left(\frac{\|\tilde{\mathcal{X}} - \mathcal{X}^*\|}{n_1 n_2 n_3} \geq \frac{1}{8} \min \left\{ (1 - \varsigma)^2 b^2, \frac{\beta_a^2 \zeta r n_1 n_3}{m} \right\} \right) \geq \tilde{\theta}_1, \end{aligned} \quad (69)$$

where

$$\tilde{\theta}_1 = \frac{\sqrt{|\tilde{\mathfrak{X}}_{\mathcal{A}}^0| - 1}}{1 + \sqrt{|\tilde{\mathfrak{X}}_{\mathcal{A}}^0| - 1}} \left(1 - 2\tilde{\alpha}_1 - \sqrt{\frac{2\tilde{\alpha}_1}{\log(|\tilde{\mathfrak{X}}_{\mathcal{A}}^0| - 1)}} \right) \in (0, 1).$$

Similar to the previous discussion, we define a subset $\tilde{\mathfrak{X}}_{\mathcal{B}} \subseteq \mathbb{R}^{n_1 \times n_2 \times n_3}$ as

$$\tilde{\mathfrak{X}}_{\mathcal{B}} := \left\{ \mathcal{X} = (\mathcal{A}_0 + \mathcal{A}_1) \diamond \mathcal{B} : \mathcal{B} \in \tilde{\mathfrak{B}}_1 \right\}, \quad (70)$$

where

$$\mathcal{A}_0 := (\mathcal{M}_1 \mathbf{0}) \in \mathbb{R}^{n_1 \times r \times n_3} \text{ with } \mathcal{M}_1 \in \mathbb{R}^{n_1 \times 1 \times n_3},$$

and

$$\mathcal{A}_1 := \begin{pmatrix} \mathbf{0}_{r'1} & \mathcal{I}_{r'} & \mathbf{0} \\ \vdots & \vdots & \vdots \\ \mathbf{0}_{r'1} & \mathcal{I}_{r'} & \mathbf{0} \\ \mathbf{0}_{r'1} & \mathbf{0} & \mathbf{0} \end{pmatrix} \in \mathbb{R}^{n_1 \times r \times n_3}.$$

Here $\mathbf{0}_{r'1} \in \mathbb{R}^{r' \times 1 \times n_3}$ is a zero tensor, and $\mathcal{I}_{r'} \in \mathbb{R}^{r' \times r' \times n_3}$ is the identity tensor, $\mathcal{M}_1 \in \mathbb{R}^{n_1 \times 1 \times n_3}$ denotes a tensor that the first frontal slice is all one and other frontal slices are zeros. $\tilde{\mathfrak{B}}_1 \subseteq \mathfrak{B}_1$ is defined as

$$\tilde{\mathfrak{B}}_1 := \left\{ \mathcal{B} = \begin{pmatrix} \zeta \mathbb{I}_1 \\ \mathcal{B}_{r'} \\ \mathbf{0} \end{pmatrix}, \mathbb{I}_1 \in \mathbb{R}^{1 \times n_2 \times n_3}, \mathcal{B}_{r'} \in \mathbb{R}^{r' \times n_2 \times n_3}, (\mathcal{B}_{r'})_{ijk} \in \{0, b_0\}, \|\mathcal{B}_{r'}\|_0 \leq s - n_2 n_3 \right\}, \quad (71)$$

where $r' = \lceil \frac{s}{n_2 n_3} \rceil - 1$ and \mathbb{I}_1 represents a tensor with all entries being ones. By the definition of tensor-tensor product and the structure of \mathcal{A}_1 , we get that $\mathcal{A}_1 \diamond \mathcal{B} = \mathcal{A}_1 \diamond \mathcal{B}'$. For any $\mathcal{X} \in \tilde{\mathfrak{X}}_{\mathcal{B}}$, we have

$$\begin{aligned}
\mathcal{X} &= \mathcal{A}_0 \diamond \mathcal{B} + \mathcal{A}_1 \diamond \mathcal{B} \\
&= \text{Fold} \left(\begin{pmatrix} \mathbf{N}_{n_1 r} & \mathbf{0} & \cdots & \mathbf{0} \\ \mathbf{0} & \mathbf{N}_{n_1 r} & \cdots & \mathbf{0} \\ \vdots & \vdots & \ddots & \vdots \\ \mathbf{0} & \mathbf{0} & \cdots & \mathbf{N}_{n_1 r} \end{pmatrix} \cdot \begin{pmatrix} \mathbf{B}^{(1)} \\ \mathbf{B}^{(2)} \\ \vdots \\ \mathbf{B}^{(n_3)} \end{pmatrix} \right) + \mathcal{A}_1 \diamond \mathcal{B}' \\
&= \text{Fold} \begin{pmatrix} \zeta \mathbf{E}_{n_1 n_2} \\ \zeta \mathbf{E}_{n_1 n_2} \\ \vdots \\ \zeta \mathbf{E}_{n_1 n_2} \end{pmatrix} + \mathcal{A}_1 \diamond \mathcal{B}' \\
&= \zeta \mathbb{I}_n + \mathcal{A}_1 \diamond \mathcal{B}',
\end{aligned} \tag{72}$$

where $\mathbf{N}_{n_1 r} = (\mathbf{E}_{n_1 1} \ \mathbf{0}_{n_1(r-1)}) \in \mathbb{R}^{n_1 \times r}$ with $\mathbf{E}_{n_1 1} \in \mathbb{R}^{n_1 \times 1}$ being a column vector (all 1),

$$\mathbf{B}^{(i)} = \begin{pmatrix} \zeta \mathbf{E}_{1 n_2} \\ \mathbf{B}_{r'}^{(i)} \\ \mathbf{0} \end{pmatrix}$$

with $\mathbf{E}_{1 n_2} \in \mathbb{R}^{1 \times n_2}$ being a row vector (all 1) and $\mathbf{B}_{r'}^{(i)}$ being the i th frontal slice of $\mathcal{B}_{r'}$, $\mathbb{I}_n \in \mathbb{R}^{n_1 \times n_2 \times n_3}$ is a tensor with all entries being 1, and

$$\mathcal{B}' = \begin{pmatrix} \mathbf{0}_1 \\ \mathcal{B}_{r'} \\ \mathbf{0} \end{pmatrix}$$

with $\mathbf{0}_1 \in \mathbb{R}^{1 \times n_2 \times n_3}$ being a zero tensor. Therefore, $\mathcal{X} \in \tilde{\mathfrak{U}}(r, b, s, \zeta)$, which implies that $\tilde{\mathfrak{X}}_{\mathcal{B}} \subseteq \tilde{\mathfrak{U}}(r, b, s, \zeta)$. Therefore, by applying the Varshamov-Gilbert bound [55, Lemma 2.9] to the last term of (72), for any $\mathcal{X}_1, \mathcal{X}_2 \in \tilde{\mathfrak{X}}_{\mathcal{B}}^0$, there exists a subset $\tilde{\mathfrak{X}}_{\mathcal{B}}^0 \subseteq \tilde{\mathfrak{X}}_{\mathcal{B}}$ such that $|\tilde{\mathfrak{X}}_{\mathcal{B}}^0| \geq 2^{\frac{s-n_2 n_3}{8}} + 1$

$$\begin{aligned}
\|\mathcal{X}_1 - \mathcal{X}_2\|_F^2 &\geq \left(\frac{s - n_2 n_3}{8} \right) \left\lfloor \frac{n_1}{r'} \right\rfloor b_0^2 \\
&\geq \left(\frac{s - n_2 n_3}{16} \right) \cdot \frac{n_1}{r'} \cdot \min \left\{ b^2, \beta_b^2 \frac{\zeta}{\Delta_1} \frac{s - n_2 n_3}{m} \right\} \\
&\geq \frac{n_1 n_2 n_3}{32} \Delta_1 \min \left\{ b^2, \beta_b^2 \frac{\zeta}{\Delta_1} \frac{s - n_2 n_3}{m} \right\} \\
&= \frac{n_1 n_2 n_3}{32} \min \left\{ \Delta_1 b^2, \beta_b^2 \zeta \frac{s - n_2 n_3}{m} \right\},
\end{aligned}$$

where the third inequality holds by the fact that $\frac{x}{|x|} \geq \min\{\frac{1}{2}, x\}$ for any $x > 0$. The KL divergence of $p_{\mathcal{X}_\Omega}(\mathcal{Y}_\Omega)$ from $p_{(\mathcal{X}_0)_\Omega}(\mathcal{Y}_\Omega)$ is

$$\begin{aligned} D(p_{\mathcal{X}_\Omega}(\mathcal{Y}_\Omega) || p_{(\mathcal{X}_0)_\Omega}(\mathcal{Y}_\Omega)) &= \frac{m}{n_1 n_2 n_3} \sum_{i,j,k} D(p_{\mathcal{X}_{ijk}}(\mathcal{Y}_{ijk}) || p_{(\mathcal{X}_0)_{ijk}}(\mathcal{Y}_{ijk})) \\ &\leq \frac{m}{n_1 n_2 n_3} \sum_{i,j,k} \frac{(\mathcal{X}_{ijk} - \zeta)^2}{\zeta} \\ &\leq m \frac{b_0^2}{\zeta} \Delta_1 \leq \beta_b^2 (s - n_2 n_3) \leq \frac{8\beta_b^2 \log(|\mathfrak{X}_B^0| - 1)}{\log(2)}, \end{aligned}$$

where the second inequality follows from $\|\mathcal{A}_1 \diamond \mathcal{B}'\|_0 \leq \lfloor \frac{n_1}{r'} \rfloor (s - n_2 n_3) \leq n_1 n_2 n_3 \Delta_1$ and the last inequality follows from $|\tilde{\mathfrak{X}}_B^0| \geq 2^{\frac{s-n_2 n_3}{s}} + 1$. Therefore, by choosing $0 < \beta_b \leq \frac{\sqrt{\tilde{\alpha}_2 \log(2)}}{2\sqrt{2}}$ with $0 < \tilde{\alpha}_2 < 1/8$, we have

$$\frac{1}{|\mathfrak{X}_B^0| - 1} \sum_{\mathcal{X} \in \mathfrak{X}_B^0} D(p_{\mathcal{X}_\Omega}(\mathcal{Y}_\Omega) || p_{(\mathcal{X}_0)_\Omega}(\mathcal{Y}_\Omega)) \leq \tilde{\alpha}_2 \log(|\mathfrak{X}_B^0| - 1).$$

By [55, Theorem 2.5], we obtain that

$$\begin{aligned} &\inf_{\tilde{\mathcal{X}}} \sup_{\mathcal{X}^* \in \tilde{\mathfrak{X}}_B} \mathbb{P} \left(\frac{\|\tilde{\mathcal{X}} - \mathcal{X}^*\|_F^2}{n_1 n_2 n_3} \geq \frac{1}{32} \min \left\{ \Delta_1 b^2, \beta_b^2 \zeta \frac{s - n_2 n_3}{m} \right\} \right) \\ &\geq \inf_{\tilde{\mathcal{X}}} \sup_{\mathcal{X}^* \in \tilde{\mathfrak{X}}_B^0} \mathbb{P} \left(\frac{\|\tilde{\mathcal{X}} - \mathcal{X}^*\|}{n_1 n_2 n_3} \geq \frac{1}{32} \min \left\{ \Delta_1 b^2, \beta_b^2 \zeta \frac{s - n_2 n_3}{m} \right\} \right) \geq \tilde{\theta}_2, \end{aligned} \quad (73)$$

where

$$\tilde{\theta}_2 = \frac{\sqrt{|\tilde{\mathfrak{X}}_B^0| - 1}}{1 + \sqrt{|\tilde{\mathfrak{X}}_B^0| - 1}} \left(1 - 2\tilde{\alpha}_2 - \sqrt{\frac{2\tilde{\alpha}_2}{\log(|\tilde{\mathfrak{X}}_B^0| - 1)}} \right) \in (0, 1).$$

By combining (69) and (73), we deduce

$$\inf_{\tilde{\mathcal{X}}} \sup_{\mathcal{X}^* \in \mathfrak{U}(r, b, k)} \mathbb{P} \left(\frac{\|\tilde{\mathcal{X}} - \mathcal{X}^*\|_F^2}{n_1 n_2 n_3} \geq \frac{1}{64} \min \left\{ \tilde{\Delta} b^2, \tilde{\beta}_c^2 \zeta \left(\frac{s - n_2 n_3 + r n_1 n_3}{m} \right) \right\} \right) \geq \tilde{\theta}_c,$$

where $\tilde{\Delta} := \min\{(1 - \zeta)^2, \Delta_1\}$, $\tilde{\beta}_c := \{\beta_a, \beta_b\}$, and $\tilde{\theta}_c = \min\{\tilde{\theta}_1, \tilde{\theta}_2\}$. By Markov's inequality, the desired conclusion is obtained easily.

REFERENCES

- [1] T. G. Kolda and B. W. Bader, "Tensor decompositions and applications," *SIAM Rev.*, vol. 51, no. 3, pp. 455–500, 2009.
- [2] T. G. Kolda and J. Sun, "Scalable tensor decompositions for multi-aspect data mining," in *2008 Eighth IEEE Int. Conf. Data Mining*, 2008, pp. 363–372.
- [3] M. Mørup, "Applications of tensor (multiway array) factorizations and decompositions in data mining," *Wiley Interdisciplinary Reviews: Data Mining and Knowledge Discovery*, vol. 1, no. 1, pp. 24–40, 2011.
- [4] A. Cichocki, R. Zdunek, and S.-i. Amari, "Nonnegative matrix and tensor factorization [lecture notes]," *IEEE Signal Process. Mag.*, vol. 25, no. 1, pp. 142–145, 2008.

- [5] A. Cichocki, D. Mandic, L. De Lathauwer, G. Zhou, Q. Zhao, C. Caiafa, and H. A. Phan, "Tensor decompositions for signal processing applications: From two-way to multiway component analysis," *IEEE Signal Process. Mag.*, vol. 32, no. 2, pp. 145–163, Mar. 2015.
- [6] N. D. Sidiropoulos, L. De Lathauwer, X. Fu, K. Huang, E. E. Papalexakis, and C. Faloutsos, "Tensor decomposition for signal processing and machine learning," *IEEE Trans. Signal Process.*, vol. 65, no. 13, pp. 3551–3582, Jul. 2017.
- [7] X. Zhang, "A nonconvex relaxation approach to low-rank tensor completion," *IEEE Trans. Neural Netw. Learn. Syst.*, vol. 30, no. 6, pp. 1659–1671, Jun. 2019.
- [8] S. Mori and J. Zhang, "Principles of diffusion tensor imaging and its applications to basic neuroscience research," *Neuron*, vol. 51, no. 5, pp. 527–539, 2006.
- [9] C. H. Ding, T. Li, and M. I. Jordan, "Convex and semi-nonnegative matrix factorizations," *IEEE Trans. Pattern Anal. Mach. Intell.*, vol. 32, no. 1, pp. 45–55, Jan. 2010.
- [10] D. D. Lee and H. S. Seung, "Learning the parts of objects by non-negative matrix factorization," *Nature*, vol. 401, no. 6755, pp. 788–791, 1999.
- [11] N. Gillis, *Nonnegative Matrix Factorization*. SIAM, Philadelphia, PA, 2020.
- [12] J. Pan and N. Gillis, "Generalized separable nonnegative matrix factorization," *IEEE Trans. Pattern Anal. Mach. Intell.*, vol. 43, no. 5, pp. 1546–1561, May 2021.
- [13] J. Pan and M. K. Ng, "Orthogonal nonnegative matrix factorization by sparsity and nuclear norm optimization," *SIAM J. Matrix Anal. Appl.*, vol. 39, no. 2, pp. 856–875, 2018.
- [14] N. Gillis, "Sparse and unique nonnegative matrix factorization through data preprocessing," *J. Mach. Learn. Res.*, vol. 13, no. 108, pp. 3349–3386, 2012.
- [15] Y. Gao and G. Church, "Improving molecular cancer class discovery through sparse non-negative matrix factorization," *Bioinformatics*, vol. 21, no. 21, pp. 3970–3975, 2005.
- [16] R. Zhi, M. Flierl, Q. Ruan, and W. B. Kleijn, "Graph-preserving sparse nonnegative matrix factorization with application to facial expression recognition," *IEEE Trans. Syst., Man, Cybern. B, Cybern.*, vol. 41, no. 1, pp. 38–52, Feb. 2011.
- [17] N. Gillis and F. Glineur, "Using underapproximations for sparse nonnegative matrix factorization," *Pattern Recognit.*, vol. 43, no. 4, pp. 1676–1687, 2010.
- [18] H. Kim and H. Park, "Sparse non-negative matrix factorizations via alternating non-negativity-constrained least squares for microarray data analysis," *Bioinformatics*, vol. 23, no. 12, pp. 1495–1502, 2007.
- [19] S. Soltani, M. S. Andersen, and P. C. Hansen, "Tomographic image reconstruction using training images," *J. Comput. Appl. Math.*, vol. 313, pp. 243–258, Mar. 2017.
- [20] A. Soni, S. Jain, J. Haupt, and S. Gonella, "Noisy matrix completion under sparse factor models," *IEEE Trans. Inf. Theory*, vol. 62, no. 6, pp. 3636–3661, Jun. 2016.
- [21] A. V. Sambasivan and J. D. Haupt, "Minimax lower bounds for noisy matrix completion under sparse factor models," *IEEE Trans. Inf. Theory*, vol. 64, no. 5, pp. 3274–3285, Mar. 2018.
- [22] E. C. Chi and T. G. Kolda, "On tensors, sparsity, and nonnegative factorizations," *SIAM J. Matrix Anal. Appl.*, vol. 33, no. 4, pp. 1272–1299, 2012.
- [23] D. Hong, T. G. Kolda, and J. A. Dueresch, "Generalized canonical polyadic tensor decomposition," *SIAM Rev.*, vol. 62, no. 1, pp. 133–163, 2020.
- [24] M. Mørup, L. K. Hansen, and S. M. Arnfred, "Algorithms for sparse nonnegative Tucker decompositions," *Neural Comput.*, vol. 20, no. 8, pp. 2112–2131, 2008.
- [25] J. Pan, M. K. Ng, Y. Liu, X. Zhang, and H. Yan, "Orthogonal nonnegative Tucker decomposition," *SIAM J. Sci. Comput.*, vol. 43, no. 1, pp. B55–B81, 2021.
- [26] M. A. Veganzones, J. E. Cohen, R. C. Farias, J. Chanussot, and P. Comon, "Nonnegative

- tensor CP decomposition of hyperspectral data,” *IEEE Trans. Geosci. Remote Sens.*, vol. 54, no. 5, pp. 2577–2588, May 2016.
- [27] X. Li, M. K. Ng, G. Cong, Y. Ye, and Q. Wu, “MR-NTD: Manifold regularization nonnegative Tucker decomposition for tensor data dimension reduction and representation,” *IEEE Trans. Neural Netw. Learn. Syst.*, vol. 28, no. 8, pp. 1787–1800, Aug. 2017.
 - [28] N. Lee, A.-H. Phan, F. Cong, and A. Cichocki, “Nonnegative tensor train decompositions for multi-domain feature extraction and clustering,” in *Int. Conf. Neural Inform. Process.*, 2016, pp. 87–95.
 - [29] N. Vervliet, O. Debals, and L. De Lathauwer, “Exploiting efficient representations in large-scale tensor decompositions,” *SIAM J. Sci. Comput.*, vol. 41, no. 2, pp. A789–A815, 2019.
 - [30] Y. Xu, “Alternating proximal gradient method for sparse nonnegative Tucker decomposition,” *Math. Program. Comput.*, vol. 7, no. 1, pp. 39–70, 2015.
 - [31] N. Qi, Y. Shi, X. Sun, J. Wang, B. Yin, and J. Gao, “Multi-dimensional sparse models,” *IEEE Trans. Pattern Anal. Mach. Intell.*, vol. 40, no. 1, pp. 163–178, Jan. 2018.
 - [32] H.-J. Kim, E. Ollila, and V. Koivunen, “Sparse regularization of tensor decompositions,” in *2013 IEEE Int. Conf. Acoustics, Speech and Signal Process.*, 2013, pp. 3836–3840.
 - [33] M. E. Kilmer and C. D. Martin, “Factorization strategies for third-order tensors,” *Linear Algebra Appl.*, vol. 435, no. 3, pp. 641–658, 2011.
 - [34] M. E. Kilmer, K. Braman, N. Hao, and R. C. Hoover, “Third-order tensors as operators on matrices: A theoretical and computational framework with applications in imaging,” *SIAM J. Matrix Anal. Appl.*, vol. 34, no. 1, pp. 148–172, 2013.
 - [35] C. D. Martin, R. Shafer, and B. Larue, “An order-p tensor factorization with applications in imaging,” *SIAM J. Sci. Comput.*, vol. 35, no. 1, pp. A474–A490, 2013.
 - [36] G. Song, M. K. Ng, and X. Zhang, “Robust tensor completion using transformed tensor singular value decomposition,” *Numer. Linear Algebra Appl.*, vol. 27, no. 3, p. e2299, 2020.
 - [37] N. Hao, M. E. Kilmer, K. Braman, and R. C. Hoover, “Facial recognition using tensor-tensor decompositions,” *SIAM J. Imaging Sci.*, vol. 6, no. 1, pp. 437–463, 2013.
 - [38] M. K. Ng, X. Zhang, and X.-L. Zhao, “Patched-tubes unitary transform for robust tensor completion,” *Pattern Recognit.*, vol. 100, p. 107181, Apr. 2020.
 - [39] X. Zhang and M. K. Ng, “A corrected tensor nuclear norm minimization method for noisy low-rank tensor completion,” *SIAM J. Imaging Sci.*, vol. 12, no. 2, pp. 1231–1273, 2019.
 - [40] Z. Zhang, G. Ely, S. Aeron, N. Hao, and M. Kilmer, “Novel methods for multilinear data completion and de-noising based on tensor-SVD,” in *Proc. IEEE Conf. Comput. Vision Pattern Recognit.*, 2014, pp. 3842–3849.
 - [41] Z. Zhang and S. Aeron, “Exact tensor completion using t-SVD,” *IEEE Trans. Signal Process.*, vol. 65, no. 6, pp. 1511–1526, Mar. 2017.
 - [42] X. Zhang and M. K. Ng, “Low rank tensor completion with Poisson observations,” *IEEE Trans. Pattern Anal. Mach. Intell.*, DOI: 10.1109/TPAMI.2021.3059299, Feb. 2021.
 - [43] O. Semerci, N. Hao, M. E. Kilmer, and E. L. Miller, “Tensor-based formulation and nuclear norm regularization for multienergy computed tomography,” *IEEE Trans. Image Process.*, vol. 23, no. 4, pp. 1678–1693, Apr. 2014.
 - [44] Y.-B. Zheng, T.-Z. Huang, X.-L. Zhao, T.-X. Jiang, T.-H. Ma, and T.-Y. Ji, “Mixed noise removal in hyperspectral image via low-fibered-rank regularization,” *IEEE Trans. Geosci. Remote Sens.*, vol. 58, no. 1, pp. 734–749, Jan. 2020.
 - [45] S. Soltani, M. E. Kilmer, and P. C. Hansen, “A tensor-based dictionary learning approach to tomographic image reconstruction,” *BIT Numer. Math.*, vol. 56, no. 4, pp. 1425–1454, 2016.

- [46] E. Newman and M. E. Kilmer, “Non-negative tensor patch dictionary approaches for image compression and deblurring applications,” *SIAM J. Imaging Sci.*, vol. 13, no. 3, pp. 1084–1112, 2020.
- [47] D. Gabay and B. Mercier, “A dual algorithm for the solution of nonlinear variational problems via finite element approximation,” *Comput. Math. Appl.*, vol. 2, no. 1, pp. 17–40, 1976.
- [48] Y. Wang, W. Yin, and J. Zeng, “Global convergence of ADMM in nonconvex nonsmooth optimization,” *J. Sci. Comput.*, vol. 78, no. 1, pp. 29–63, 2019.
- [49] M. Raginsky, R. M. Willett, Z. T. Harmany, and R. F. Marcia, “Compressed sensing performance bounds under Poisson noise,” *IEEE Trans. Signal Process.*, vol. 58, no. 8, pp. 3990–4002, Aug. 2010.
- [50] B. McMillan, “Two inequalities implied by unique decipherability,” *IEEE Trans. Inf. Theory*, vol. 2, no. 4, pp. 115–116, Dec. 1956.
- [51] L. G. Kraft, “A device for quantizing, grouping, and coding amplitude-modulated pulses,” M.S. Thesis, Massachusetts Institute of Technology, 1949.
- [52] A. Wang, Z. Lai, and Z. Jin, “Noisy low-tubal-rank tensor completion,” *Neurocomputing*, vol. 330, pp. 267–279, Feb. 2019.
- [53] Y. Cao and Y. Xie, “Poisson matrix recovery and completion,” *IEEE Trans. Signal Process.*, vol. 64, no. 6, pp. 1609–1620, Mar. 2016.
- [54] O. Klopp, K. Lounici, and A. B. Tsybakov, “Robust matrix completion,” *Probab. Theory Relat. Fields*, vol. 169, no. 1-2, pp. 523–564, 2017.
- [55] A. B. Tsybakov, *Introduction to Nonparametric Estimation*. Springer, New York, 2009.
- [56] M. Hong, Z. Q. Luo, and M. Razaviyayn, “Convergence analysis of alternating direction method of multipliers for a family of nonconvex problems,” *SIAM J. Optim.*, vol. 26, no. 1, pp. 337–364, 2016.
- [57] D. L. Donoho and J. M. Johnstone, “Ideal spatial adaptation by wavelet shrinkage,” *Biometrika*, vol. 81, no. 3, pp. 425–455, 1994.
- [58] A. Beck, *First-Order Methods in Optimization*. SIAM: Philadelphia, 2017.
- [59] B. W. Bader, T. G. Kolda *et al.*, “MATLAB Tensor Toolbox, Version 3.1,” Available online: <https://www.tensortoolbox.org>, 2019.
- [60] C. Zeng and M. K. Ng, “Decompositions of third-order tensors: HOSVD, T-SVD, and beyond,” *Numer. Linear Algebra Appl.*, vol. 27, no. 3, p. e2290, 2020.
- [61] Q. J. Li, “Estimation of mixture models,” Ph.D. Thesis, Yale University, 1999.
- [62] T. M. Cover and J. A. Thomas, *Elements of Information Theory*. 2nd Edition, John Wiley & Sons, New Jersey, 2006.
- [63] M. J. Wainwright, *High-Dimensional Statistics: A Non-Asymptotic Viewpoint*. Cambridge University Press, Cambridge, 2019.
- [64] A. V. Carter, “Deficiency distance between multinomial and multivariate normal experiments,” *Ann. Statist.*, vol. 30, no. 3, pp. 708–730, 2002.